SIAM J. MATH. ANAL.
Vol. 55, No. 5, pp. 4219–4254

EDGE STATE DYNAMICS ALONG CURVED INTERFACES*

GUILLAUME BAL†, SIMON BECKER‡, ALEXIS DROUOT§, CLOTILDE FERMANIAN KAMMERER¶, JIANFENG LU‖, AND ALEXANDER B. WATSON#

Abstract. We study the propagation of wavepackets along weakly curved interfaces between topologically distinct media. Our Hamiltonian is an adiabatic modulation of Dirac operators omnipresent in the topological insulators literature. Using explicit formulas for straight edges, we construct a family of solutions that propagates, for long times, unidirectionally and dispersion-free along the curved edge. We illustrate our results through various numerical simulations.

Key words. Dirac equation, quantum mechanics, topological insulators, edge states

MSC codes. 81Q10, 81Q05

DOI. 10.1137/22M1489708

1. Introduction.

Topological insulators are fascinating materials that are insulating in their bulk but support robust currents along their boundary. From a qualitative point of view, these properties are explained by the bulk-edge correspondence, an index-like theorem that relates the net conductivity (an analytic index) to the bulk topology (a topological index). For straight interfaces, the currents are explicitly described in terms of edge states: steady waves with ballistic dynamics, confined between regions of distinct topology.

In this work, we construct dynamical analogues of edge states for curved interfaces. Our model is a Dirac operator

$$H = \begin{bmatrix} \kappa(x) & \varepsilon D_{x_1} - i\varepsilon D_{x_2} \\ \varepsilon D_{x_1} + i\varepsilon D_{x_2} & -\kappa(x) \end{bmatrix}, \tag{1.1}$$

where $D_{x_j} = -i\partial_{x_j}$, $\varepsilon > 0$ is a small semiclassical parameter and κ is a varying mass term. Such Hamiltonians emerge in the effective theory of honeycomb structures [18, 36, 13]; more generally they model the generic dynamics of modes propagating along interfaces between topologically distinct insulators [15]. We can interpret the parameter ε as the Fermi velocity of a Dirac cone; therefore the regime $\varepsilon \ll 1$ corresponds to nearly flat Dirac cones.

*Received by the editors April 11, 2022; accepted for publication (in revised form) February 17, 2023; published electronically September 12, 2023.
https://doi.org/10.1137/22M1489708
Funding: The authors acknowledge support form the National Science Foundation grants DMREF-1922165 (A.W.), DMS-2054589 and DMS-2118608 (A.D.), DMS-1908736 (G.B.), EFMA-1641100 (G.B.), and DMS-2012286 (J.L.); the Engineering and Physical Sciences Research Council grant EP/L016516/1 (S.B.); the U.S. Department of Energy grant DE-SC0019449 (J.L.); the Office of Naval Research grant N00014-17-1-2096 (G.B.); and the Army Research Office MURI (ARO MURI) grant W911NF-14-0247 (A.W.).

†University of Chicago, Chicago, IL 60637 USA (guillaumebal@uchicago.edu).
‡ETH Zurich, Zurich, Switzerland (simon.becker@math.ethz.ch).
§University of Washington, Seattle, WA 98195 USA (adrouot@uw.edu).
¶Univ Paris Est Créteil, Univ Gustave Eiffel, CNRS, Lama UMR8050, F-94010 Creteil, France (clotilde.fermanian@u-pec.fr).
‖Duke University, Durham, NC 27708 USA (jianfeng@math.duke.edu).
#University of Minnesota, Minneapolis, MN 55455 USA (watso860@umn.edu).

Under a transversality condition, $\nabla\kappa(x) \neq 0$ when $\kappa(x) = 0$, the set

$$\Gamma = \{x \in \mathbb{R}^2 : \kappa(x) = 0\}$$

partitions $\mathbb{R}^2$ in regions of distinct local topology; see section 1.5 for details. A local interpretation of the bulk-edge correspondence suggests that nontrivial currents emerge along Γ. This paper develops the underlying quantitative theory; it provides detailed information on the associated quantum states, such as their speed and profile.

Specifically, we exploit the explicit structure of edge states available when $\kappa(x) = a_1x_1 + a_2x_2$ to construct an infinite-dimensional family of nearly steady solutions to $(\varepsilon D_t + H)\psi = 0$, in the limit $\varepsilon \to 0$. These emerge as the natural channels of conductivity: for long times, they propagate unidirectionally and coherently along Γ. We show that the curvature of Γ plays a key role in limiting the lifetime of these solutions. We illustrate our results via various numerical simulations.

1.1. Simplified main result. Throughout the paper, we assume that all derivatives of κ (but not necessarily κ) are uniformly bounded: $\nabla\kappa \in C_b^\infty(\mathbb{R}^2)$. In this introduction, we require moreover that

$$y \in \Gamma \quad \Rightarrow \quad \big|\nabla\kappa(y)\big| = 1. \tag{1.2}$$

This allows us to state a simplified version (Theorem 1) of our main result (Theorem 2). In section 3, we replace (1.2) by the more general transversality condition (3.1).

Fix $y_0 \in \Gamma = \kappa^{-1}(0)$, and define y_t by the ODE

$$\dot{y}_t = \nabla\kappa(y_t)^\perp,$$

where $\nabla\kappa(y)^\perp$ is the tangent vector to Γ obtained by the $\pi/2$-counterclockwise rotation of $\nabla\kappa(y)$. Under (1.2), y_t is a unit speed parametrization of Γ. We let θ_t be the angle between the tangent to Γ at y_t and the x-axis; see Figure 1. We use the notation $\langle t\rangle = (1 + |t|^2)^{1/2}$.

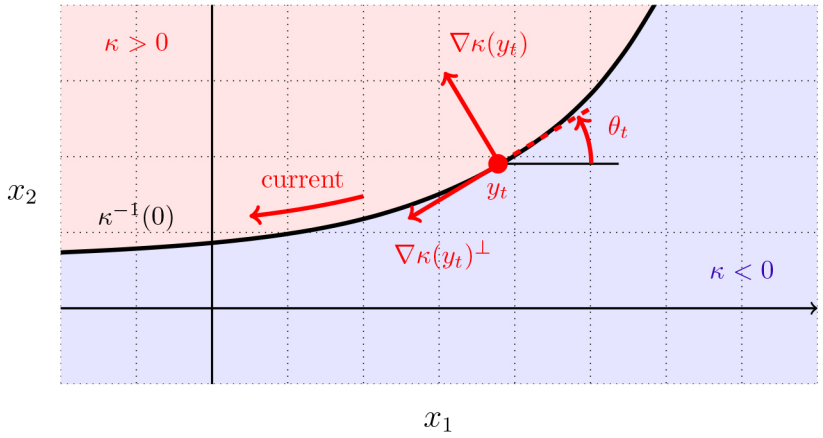

FIG. 1. *Schematic plot of an interface $\Gamma = \kappa^{-1}(0)$ between topologically distinct regions, together with y_t and θ_t.*

THEOREM 1. *Let* $\kappa \in C^\infty(\mathbb{R}^2)$ *satisfy* (1.2), *with* $\nabla\kappa \in C_b^\infty(\mathbb{R}^2)$, *and* y_t, θ_t *as above. The solution to*

$$(\varepsilon D_t + H)\Psi_t = 0, \qquad \Psi_0(x) = \frac{1}{\sqrt{\varepsilon}} \cdot \exp\left(-\frac{(x-y_0)^2}{2\varepsilon}\right) \begin{bmatrix} e^{-i\theta_0/2} \\ -e^{i\theta_0/2} \end{bmatrix} \tag{1.3}$$

satisfies, uniformly for $\varepsilon \in (0,1]$ *and* $t > 0$,

$$\Psi_t(x) = \frac{1}{\sqrt{\varepsilon}} \cdot \exp\left(-\frac{(x-y_t)^2}{2\varepsilon}\right) \begin{bmatrix} e^{-i\theta_t/2} \\ -e^{i\theta_t/2} \end{bmatrix} + \mathcal{O}_{L^2}\left(\varepsilon^{1/2}\langle t\rangle\right). \tag{1.4}$$

The initial data (1.3) are Gaussian concentrated at y_0. Theorem 1 shows that the generated solution remains (at leading order for times $t \ll \varepsilon^{-1/2}$) a Gaussian, concentrated now at y_t. This identifies $t \mapsto y_t$ as an exotic quantum trajectory; it is not predicted by the standard results on propagation of semiclassical singularities that show propagation along the Hamiltonian curves of the functions $(x,\xi) \mapsto \pm\sqrt{\kappa(x)^2 + |\xi|^2}$ (see [25, 24, 22]). Moreover, for fixed times and better-prepared initial data, the concentration near y_t is accurate up to $O(\varepsilon^\infty)$; see Theorem 3. Besides, since the classical Hamiltonian vanishes along the curve $t \mapsto (y_t, 0)$, there is no time-dependent oscillating phase, as one usually has when considering propagation of wavepackets by Schrödinger equations as in [11].

If Γ is not asymptotically straight—for instance, if it is a loop—numerical computations confirm that the Gaussian state approximation becomes less and less accurate; see Figure 2. In contrast, if Γ is asymptotically straight—as in, e.g., the tanh-like interface of Figure 3—the Gaussian state approximation can work for longer times; see Theorem 4.

We refer to Theorem 2 for a more general version of Theorem 1. It constructs an infinite-dimensional family of solutions to $(\varepsilon D_t + H)\Psi_t = 0$ with the same qualitative features as (1.4): coherent states propagating unidirectionally, at unit speed and

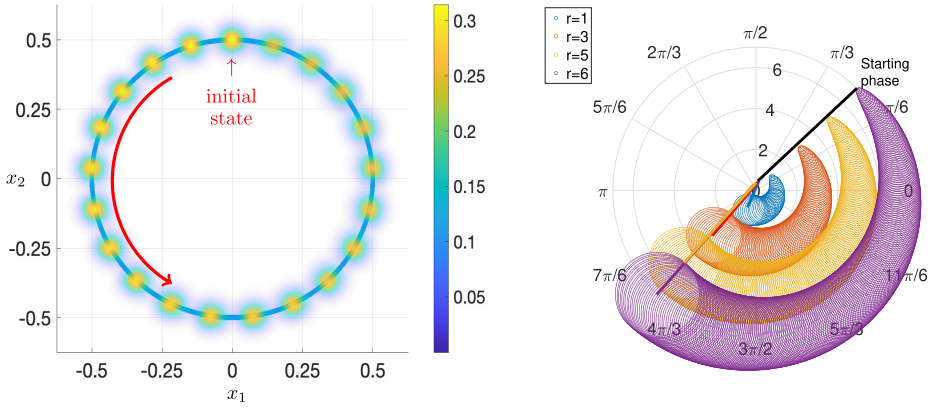

FIG. 2. *Left: numerical solution to* $(\varepsilon D_t + H)\Psi_t = 0$ *with Gaussian initial state for a circular interface with* $\varepsilon = 10^{-2}$ *and radius one. The trajectory* y_t *undergoes curvature effects for all times. This explains a dispersion stronger than for a* tanh*-type interface. See also Figure* 7 *and Theorem* 4. *Right: evolution of the phase of the first coordinate of the numerical solution for each snapshot, corresponding to* $-\theta_t/2$, *for different radii of the circle interface. After a full revolution, the numerical phase difference is about* $-\pi$, *matching the theoretical prediction* $-2\pi/2 = -\pi$. *This phase shift interprets as a Berry phase arising from adiabatically varying the parameter* θ *in the effective leading-order operator* $H_{\theta,r}$ (2.1) *from* 0 *to* 2π; *see* [46].

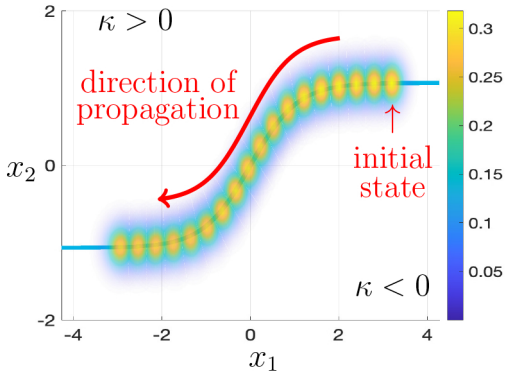

FIG. 3. *Snapshots of the numerically computed dynamical analogue of an edge state—the solution to* (1.3) *below. The interface is* $y_2 = \tanh(y_1)$ *and* $\varepsilon = 10^{-1}$. *The state propagates leftwards and dispersion-free along the interface.*

without dispersion, along Γ. Our motivation, explained in sections 1.4 and 1.5 below, is twofold:

- identify dynamical analogues of topological edge states along bent interfaces;
- study a semiclassical system whose matrix-valued symbol has repeated eigenvalues.

1.2. Numerical simulations. We illustrate our results with numerical simulations of the Dirac equation with Gaussian initial data for various types of interfaces. The corresponding pictures are snapshots of the dynamics, with the interface marked as a light blue curve.

- Figure 3 and Figure 2 are numerical confirmations of Theorem 1 for tanh-type and circle interfaces, respectively. Figure 2 also verifies that the phase shift after one revolution equals $2\pi/2 = \pi$.
- Figure 4 shows the evolution of other Gaussian states for tanh-type interfaces. The initial data are concentrated like (1.3) but carried by a different vector. If this vector is orthogonal to that in (1.3), the coherence is immediately lost. See Conjecture 1.
- When the more general transversality condition (3.1) holds instead of (1.2), the propagation is coherent in a relaxed sense. Figure 5—a straight interface but a nonlinear domain wall—numerically validates Theorem 2.
- Figure 6 illustrates the limits of the dynamical analogues of edge states; for instance, they do not propagate around sharp corners.

We use a Crank–Nicolson scheme to approximate the unitary group e^{-itH}, with Fourier spectral spatial discretization. The MATLAB code containing the parameters used to obtain our figures can be found on GitHub.[1]

1.3. Physical motivations. The Dirac equation appears in a wide variety of physical applications. Beyond its original role in the description of relativistic particles, it has emerged as a dominant model in the analysis of topological phases of matter [49, 50]. The relativistic Dirac operator ($\kappa = 0$ in our model) displays a generic band crossing; in contrast, adding a mass term opens an energy gap. In our model, the interface is the transition between the two insulating phases $\kappa < 0$ and $\kappa > 0$.

[1] https://github.com/slb2604/Semiclassical-edge-states.

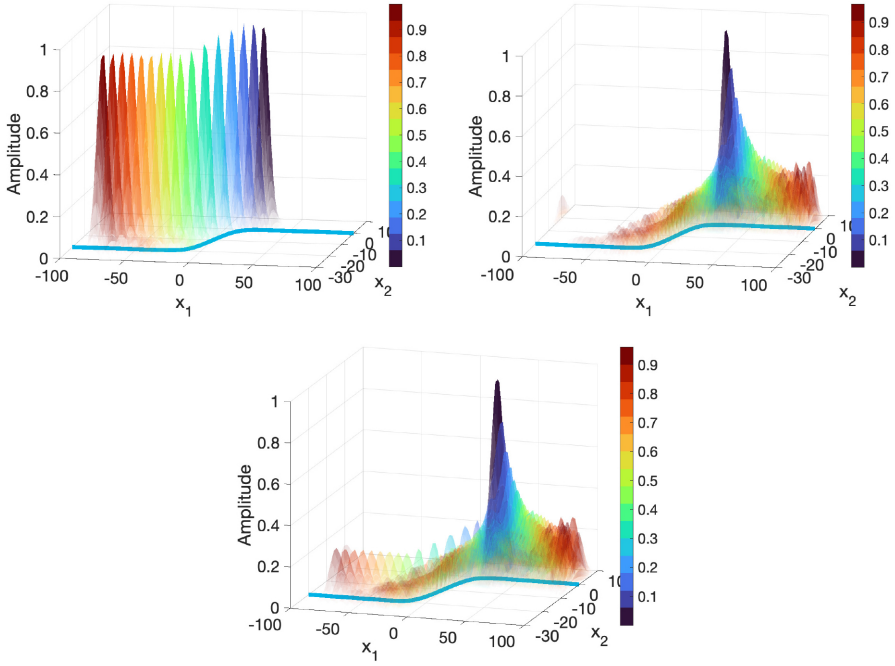

FIG. 4. *Solution to* (1.10) *for a* tanh*-like interface with (top left)* $[\alpha_1, \alpha_2] = [e^{-i\theta_0/2}, -e^{i\theta_0/2}]$, *(top right)* $[\alpha_1, \alpha_2] = [e^{-i\theta_0/2}, e^{i\theta_0/2}]$, *and (bottom)* $[\alpha_1, \alpha_2] = [0, e^{-i\theta_0/2}]$. *The top right figure corresponds to* $[\alpha_1, \alpha_2]$ *orthogonal to the vector* $[e^{-i\theta_0/2}, -e^{i\theta_0/2}]$ *from the initial data of Theorem* 1 *shown at the top left. This generates a purely dispersive wave along the interface. The bottom figure corresponds to a linear combination of the two top cases: the solution splits into leftwards-propagating and dispersive components. The color-coding is used to indicate snapshots after a time that is defined by the color.*

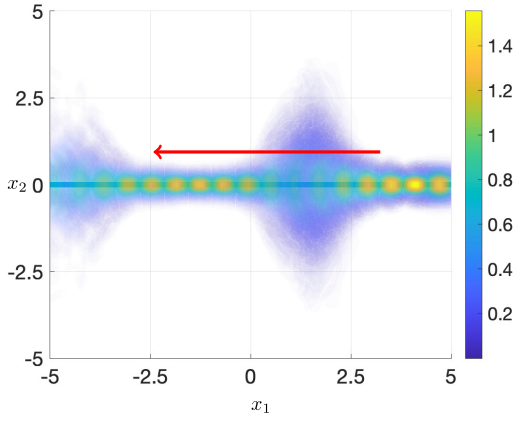

FIG. 5. *A straight interface but a nonlinear domain wall:* $\kappa(x) = (1 - 0.9\sin(x_1))x_2$. *We have* $y_t = -te_1$, *hence* $r_t = 1 + 0.9\sin(t)$. *This quantity nearly degenerates for* t *near* $-\pi/2 + \pi\mathbb{Z}$, *inducing lateral spreading of the wavepacket for such times, but reconstruction in between.*

These two phases happen to have different topological signatures; this generates unidirectional propagation along the interface.

This asymmetric transport is at the core of most physical applications in the fields of topological insulators and topological superconductors [49]. It is the

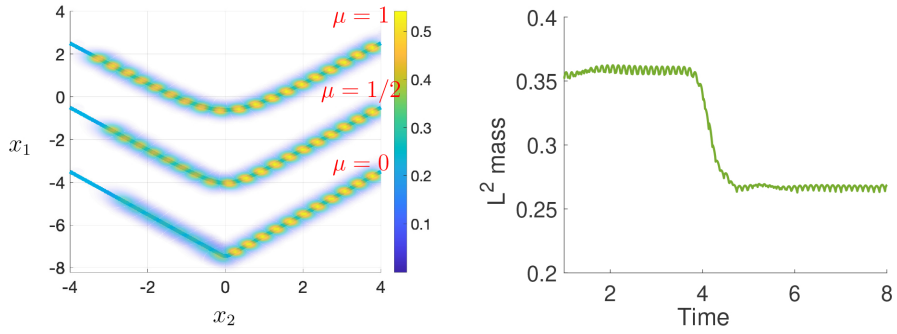

FIG. 6. *Left: Snapshots of the numerically computed solution to* $(\varepsilon D_t + H)\Psi_t = 0$, *with* $\varepsilon = 0.1$, Ψ_0 *the Gaussian* (1.4) *and a domain wall* κ, *illustrated in the figure with an appropriate offset, satisfying* (4.1), *with* $\Gamma = \{x_2 = -\sqrt{x_1^2 + \mu^2}\}$, $\mu \in \{0, 1/2, 1\}$. *The amplitude/mass loss increase as the corner gets sharper. Right:* L^2 *mass of wavepacket in* $B(y_t, \sqrt{\epsilon})$ *for* $\mu = 0$ *with visible drop at corner. Past it, about* 30% *of the mass appears to follow a dynamics different from that of the wavepacket. Additional numerical experiments suggest that this mass disperses along* Γ*; see also Conjecture* 2.

physical manifestation of the quantum Hall effect [6, 1] and its nonmagnetic analogues [9, 30, 33, 29, 37, 47]. It also finds numerous applications in fields such as photonics, acoustics, and fluid mechanics [40, 42, 44, 45, 26]. Broadly speaking, Dirac-type equations often offer the simplest continuum (macroscopic) description of transport in a narrow energy band near the band crossing [23, 49].

By interpreting ε as the Fermi velocity near Dirac cones, the regime $\varepsilon \ll 1$ corresponds to nearly flat Dirac cones. This provides a physical reason to study the equation. There is another motivation, which essentially consists in making intermediate steps toward understanding edge transport along curved interfaces. Most of the theoretical literature has focused on straight interfaces, which greatly simplifies the mathematical framework. The problem of constructing edge states along general curved interfaces has remained open. This provides a reason to study the intermediate regime of weakly curved interfaces, which is the focus of this work. Indeed, after rescaling x to εx, the interface becomes

$$\{\varepsilon^{-1} x : \kappa(x) = 0\}$$

and hence has curvature of order ε. Such interfaces behave locally like straight lines; this allows us to perform rigorous constructions of dynamical edge states. For related results, and in particular an analysis when the interface is a large circle, see [32].

This work has focused on deriving accurately a traveling state, at least for times $t \ll \varepsilon^{-1/2}$. Another line of research—somewhat transverse to this work—consists of going beyond the weakly curved regime and proving qualitative properties of currents, such as localization near the edge and scattering by sizable perturbations.

1.4. Local topological indices and asymmetric transport. Strikingly, transport at interfaces between distinct topological environments is both asymmetric (a net overall flux propagates in a prescribed direction) and quantized. We discuss here a theory of topological phases that interprets locally the state (1.4) in a topological way. We stress that this interpretation

- is valid only in the semiclassical regime $\varepsilon \ll 1$;
- is local: our construction works for all κ, even though in some scenarios H is topologically trivial (for instance, when Γ is a closed curve).

These considerations use the leading-order approximation H_y of H at a point $y \in \mathbb{R}^2$:

$$H_{\mathrm{lo}}(y) = \begin{bmatrix} \kappa(y) & \varepsilon D_{x_1} - i\varepsilon D_{x_2} \\ \varepsilon D_{x_1} + i\varepsilon D_{x_2} & -\kappa(y) \end{bmatrix}, \quad y \notin \Gamma;$$
$$H_{\mathrm{lo}}(y) = \begin{bmatrix} -v_y^{\perp} \cdot (x-y) & \varepsilon D_{x_1} - i\varepsilon D_{x_2} \\ \varepsilon D_{x_1} + i\varepsilon D_{x_2} & v_y^{\perp} \cdot (x-y) \end{bmatrix}, \quad y \in \Gamma,$$

where $v_y = \nabla\kappa(y)^{\perp}$ is tangent to Γ at y. These emerge by replacing $\kappa(x)$ in (1.1) by its leading-order development at y: $\kappa(x) \simeq \kappa(y)$ if $y \notin \Gamma$ and $\kappa(x) \simeq \nabla\kappa(y) \cdot (x-y)$ if $y \in \Gamma$. These approximations are reasonable for $|x-y| = O(\varepsilon^{1/2})$—the scale of localization of (1.4).

We observe that $H_{\mathrm{lo}}(y)$ has a spectral gap near energy 0 (i.e., it is an insulator) if and only if $y \notin \Gamma$. This identifies Γ as the natural channel for conduction of energy. Following [17, 34], we measure the local conductivity at $y \in \Gamma$ via

$$\mathcal{I}(H,y) = \mathrm{Tr}_{L^2}\left(i\big[H_{\mathrm{lo}}(y), f(v_y \cdot x)\big] g'\big(H_{\mathrm{lo}}(y)\big)\right), \qquad y \in \Gamma, \tag{1.5}$$

where f and g are smooth real functions increasing from 0 to 1 with f' and g' compactly supported. Formally,

$$\mathcal{I}(H,y) = \frac{d}{dt}\,\mathrm{Tr}_{L^2}\left(e^{itH_{\mathrm{lo}}(y)} f(v_y \cdot x) g'\big(H_{\mathrm{lo}}(y)\big) e^{-itH_{\mathrm{lo}}(y)}\right). \tag{1.6}$$

Looking at g' as a density of probability, $f(v_y \cdot x) g'(H_{\mathrm{lo}}(y))$ measures the probability of a quantum particle to lie in the half-plane $\{v_y \cdot x > 0\}$, per unit energy. Taking the trace in (1.6) corresponds to summing over all states. Hence $\mathcal{I}(H,y)$ describes the overall flux moving in the direction of v_y, per unit time and energy, at equilibrium.

It turns out that $2\pi \cdot \mathcal{I}(H,y) = 1$; see [2] and Remark 1 below. This means that the evolution according to $H_{\mathrm{lo}}(y)$ comes with a current propagating in the direction of v_y. Since v_y is tangent to Γ at y, Γ emerges intuitively as a natural charge carrier for H. Theorem 1 confirms these heuristics: in the regime $\varepsilon \to 0$, we construct a current propagating along Γ, with explicit speed and profile.

The quantity (1.5) relates to bulk topological invariants via a universal principle: the bulk-edge correspondence [31, 27, 43, 5, 14]. Following the physics literature [30, 29], we define a bulk index for $H_{\mathrm{lo}}(y)$:

$$\mathcal{B}(H,y) = \frac{\mathrm{sgn}\big(\kappa(y)\big)}{2}, \quad y \notin \Gamma. \tag{1.7}$$

When H emerges as an effective Hamiltonian (for instance, in graphene), $\mathcal{B}(H,y)$ corresponds to the integrated Berry curvature near one of the Dirac point momentum, hence as part of the overall Chern integer [12]. Direct interpretations of (1.7) as a Chern number include regularization of a Dirac operator [2] and a more general bulk-difference invariant [5]. We refer to (1.7) as the local bulk index. It can also be defined by spatially truncating physical space formulas for the global Chern number [35, 7, 43] or via the spectral localizer [38, 39].

Since $\nabla\kappa$ points from negative- to positive-index regions, we have, for $y \in \Gamma$ and $\delta > 0$ sufficiently small,

$$1 = 2\pi \cdot \mathcal{I}(H,y) = \mathcal{B}\big(H, y + \delta\nabla\kappa(y)\big) - \mathcal{B}\big(H, y - \delta\nabla\kappa(y)\big).$$

This is a local version of the bulk-edge correspondence: the local conductivity at y is the difference between the local bulk indices across the interface.

The quantity $2\pi\cdot\mathcal{I}(H,y)$ counts currents algebraically according to their direction of propagation. It is independent of y and stable against large perturbations of H; see, e.g., [2, 5] and [43] for similar models. This explains its practical significance: even in the presence of strong perturbations or Anderson localization, there is always $2\pi\cdot\mathcal{I}(H,y)=1$ more current propagating in the direction of v_y rather than $-v_y$ [3, 43]. This clarifies the *local* topological nature of the quantum state (1.4). Let us stress again that our results hold locally in time: (1.5) is spectral in nature, describing an equilibrium, while (1.4) is relevant for (long, but only transient) times $t \ll \varepsilon^{-1/2}$.

1.5. Connection with semiclassical analysis. What makes the solution (1.4) special? The answer lies in semiclassical territory. In summary (with details provided below), if $\mathcal{C}=\Gamma\times\{0\}\subset\mathbb{R}^2\times\mathbb{R}^2$, then for times $t\ll\varepsilon^{-1/2}$:

(i) states initially microlocalized at $(y_0,\xi_0)\notin\mathcal{C}$ come in pairs propagating in opposite directions;

(ii) states initially microlocalized at $(y_0,\xi_0)\in\mathcal{C}$ (i.e., like (1.3), with a potentially different 2-vector) seem to either propagate nondispersively in the direction of $\nabla\kappa^{\perp}$, or to disperse; see Figure 4 and Conjecture 1.

This suggests that Γ—more precisely, its phase-space lift $\mathcal{C}$—is the relevant channel for asymmetric propagation.

We now provide a detailed account. We start by writing $H=\mathfrak{h}(x,\varepsilon D_x)$, where

$$\mathfrak{h}(x,\xi)=\begin{bmatrix}\kappa(x) & \xi_1-i\xi_2\\ \xi_1+i\xi_2 & -\kappa(x)\end{bmatrix}.$$

Theorem 1 constructs solutions to $(\varepsilon D_t+\mathfrak{h}(x,\varepsilon D_x))\phi_t=0$ for the data

$$\phi_0(x)=\frac{1}{\sqrt{\varepsilon}}e^{\frac{i}{\varepsilon}x\cdot\xi_0}\ a\left(\frac{x-x_0}{\sqrt{\varepsilon}}\right),$$

where the profile a is a Gaussian (extended in Theorem 2 to any Schwartz profile) and where (x_0,ξ_0) belongs to the set $\mathcal{C}$ defined by

$$\mathcal{C}=\big\{(x,\xi):\ \kappa(x)=0,\ \xi=0\big\}\subset\mathbb{R}^4.$$

The function ϕ_0 is known in the literature as a semiclassical wavepacket [11] with wavefront set $WF_\varepsilon(\phi_0)=\{(x_0,\xi_0)\}$; see [51, section 8.4] for definitions and properties of wavefronts. The set $\mathcal{C}$ corresponds to semiclassical eigenvalue crossings of $\mathfrak{h}(x,\xi)$: when $(x,\xi)\in\mathcal{C}$, $\mathfrak{h}(x,\xi)$ has two degenerate eigenvalues. The systematic study of such semiclassical systems is a delicate problem. Outside the crossing set $\mathcal{C}$, for example, when $\xi_0\neq 0$, the system is *adiabatic* and the solution with initial data ϕ_0 is asymptotic to the sum of two wavepackets concentrated, respectively, on the Hamiltonian curves of the functions $(x,\xi)\mapsto\sqrt{\kappa(x)^2+|\xi|^2}$ and $(x,\xi)\mapsto-\sqrt{\kappa(x)^2+|\xi|^2}$. These trajectories never meet $\mathcal{C}$, and if $\kappa(x_0)=0$ and $\xi_0\neq 0$, the wavepacket immediately leaves the set of the zeros of κ; see [25, 24] for microlocalization of wavepackets in 4 by 4 Dirac systems and [8, 22] for a precise description of the solution in terms of wavepackets. The picture is different if one adds a potential $x\mapsto\mathfrak{u}(x)$ to the Hamiltonian $\mathfrak{h}$. In that case, Hamiltonian trajectories of the functions $(x,\xi)\mapsto\mathfrak{u}(x)\pm\sqrt{\kappa(x)^2+|\xi|^2}$ may reach $\mathcal{C}$ (see [10, 20]), which generates a Landau–Zener effect, i.e., energy transfer between the modes. These transfers have been calculated for Gaussian wavepackets and the Schrödinger equation in [28] and in terms of semiclassical measures for more

general initial data and Hamiltonians (including the case of the Dirac equation) in [21, 20, 19].

This paper focuses on the dynamics of wavepackets localized along $\mathcal{C}$ (note that the crossing energy is constant, equal to 0). One could have likewise studied the dynamics of wavepackets semiclassically concentrated at points $(x_0,\xi_0) \notin \mathcal{C}$. This is actually a much more standard problem because the eigenvalues of $\mathfrak{h}(x_0,\xi_0)$ are distinct; they are $\pm\lambda(x_0,\xi_0)$, where

$$\lambda(x,\xi) = \sqrt{\kappa(x)^2 + \xi_1^2 + \xi_2^2};$$

we note that λ does not vanish away from $\mathcal{C}$. We diagonalize $\mathfrak{h}(x,\xi)$ for (x,ξ) near (x_0,ξ_0):

$$\mathfrak{h}(x,\xi) = \mathfrak{U}(x,\xi) \begin{bmatrix} -\lambda(x,\xi) & 0 \\ 0 & \lambda(x,\xi) \end{bmatrix} \mathfrak{U}(x,\xi)^{-1},$$

where $\mathfrak{U}$ is a unitary 2×2 matrix that depends smoothly on (x,ξ). Thus, after quantization, the system $(\varepsilon D_t + \mathfrak{h}(x,\varepsilon D_x))\psi = 0$ splits semiclassically near (x_0,ξ_0) in two nearly decoupled equations [48, 41]:

$$\left(\varepsilon D_t + \begin{bmatrix} -\lambda(x,\varepsilon D_x) & 0 \\ 0 & \lambda(x,\varepsilon D_x) \end{bmatrix} + \mathcal{O}(\varepsilon)\right) \begin{bmatrix} \phi_+ \\ \phi_- \end{bmatrix} = 0.$$

According to the classical-to-quantum correspondence, the wavefront set of ϕ_t follows the semiclassical trajectories of $\pm\lambda(x,\xi)$; see, e.g., [51, Theorem 12.5]. These form two branches (x_t^+,ξ_t^+) and (x_t^-,ξ_t^-) that solve, respectively,

$$\frac{dx_t^\pm}{dt} = \pm\frac{\partial\lambda}{\partial\xi}\left(x_t^\pm,\xi_t^\pm\right), \qquad \frac{d\xi_t^\pm}{dt} = \mp\frac{\partial\lambda}{\partial x}\left(x_t^\pm,\xi_t^\pm\right). \tag{1.8}$$

The Hamiltonian trajectories (1.8) never reach $\mathcal{C}$ because (a) the energy $\pm\lambda(x_0,\xi_0) \neq 0$ is conserved along them and (b) $\mathcal{C}$ is the zero set of the function λ. Hence, if $(x_0,\xi_0) \notin \mathcal{C}$, then the semiclassical singularities of ϕ_t globally evolve according to the classical-to-quantum correspondence: they follow the Hamiltonian trajectories (1.8) and never reach $\mathcal{C}$.

Moreover, the two branches in (1.8) point (at $t = 0$) in opposite directions: wavepackets concentrated away from $\mathcal{C}$ have no preferred direction of propagation. Their contribution to an overall quantum flux cancel out. Hence, $\mathcal{C}$ is the only phase-space channel that can support unidirectional waves.

This discussion connects various characterizations of the set $\mathcal{C}$:

(i) *Semiclassical:* $\mathcal{C}$ is the set of eigenvalue crossings of $\mathfrak{h}(x,\xi)$.

(ii) *Energetic:* $\mathcal{C}$ is the characteristic set of $\mathfrak{h}(x,\xi)$, i.e., the set of points (x,ξ) such that $\det \mathfrak{h}(x,\xi) = 0$.

(iii) *Topological:* the local Chern number is not defined on $\Gamma = \kappa^{-1}(0) = \pi(\mathcal{C})$ (with $\pi(x,\xi) = x$) because the eigenvalues of $\mathfrak{h}(x,\xi)$ are degenerate on $\mathcal{C}$.

(iv) *Dynamical:* Among phase-space subsets, $\mathcal{C}$ is the only (maximal) candidate that may support unidirectional wavepackets.

Because of (i), the classical-to-quantum correspondence fails. Because of conservation of energy, (ii) suggests that a state semiclassically concentrated along $\mathcal{C}$ should remain this way: $\mathcal{C}$ acts as a semiclassical waveguide. Theorem 1 provides the corresponding profile and speed. Under global assumptions on κ, the bulk-edge correspondence predicts a nonvanishing quantum flux between regions of different topology.

From (iii), $\mathcal{C}$ acts as the natural topological interface in phase-space. According to (iv), it is also the only channel that can support waves contributing to a nontrivial conductivity.

A legitimate criticism to Theorem 1 is that it does not study the dynamics of all initial data localized along $\mathcal{C}$: it focuses on those parallel to the two-vector $[e^{-i\theta_0}, -e^{i\theta_0}]^\top$. As demonstrated numerically in Figure 4 the data prepared along the orthogonal two-vector $[-e^{i\theta_0}, e^{-i\theta_0}]^\top$ appear to purely disperse along the interface. An investigation of case κ linear suggests that the rate of dispersion is $\varepsilon^{-1/4}t^{-1/2}$: wavepackets supported by such spinors and amplitude $\varepsilon^{-1/2}$ experience a strong loss of coherence. For positive times, their peak is divided by a factor of order $\varepsilon^{-1/4}$.

Thus, we conjecture that general initial data semiclassically localized along $\mathcal{C}$ transit to the state (1.4). To write a precise statement, we split vectors $[\alpha_1, \alpha_2]^\top \in \mathbb{C}^2$ according to

$$\begin{bmatrix}\alpha_1\\ \alpha_2\end{bmatrix} = \lambda_1 \begin{bmatrix}e^{-i\theta_0/2}\\ -e^{i\theta_0/2}\end{bmatrix} + \lambda_2 \begin{bmatrix}e^{-i\theta_0/2}\\ e^{i\theta_0/2}\end{bmatrix}. \tag{1.9}$$

We interpret the two terms in (1.9) as projections on the vector from (1.3) and its orthogonal.

CONJECTURE 1. *Fix $y_0 \in \Gamma$, $\alpha_1, \alpha_2 \in \mathbb{C}$, and λ_1, λ_2 defined according to* (1.9). *Under* (1.2), *the solution Ψ_t to*

$$(\varepsilon D_t + H)\Psi_t = 0, \qquad \Psi_0(x) = \frac{1}{\sqrt{\varepsilon}} \cdot \exp\left(-\frac{|x-y_0|^2}{2\varepsilon}\right)\begin{bmatrix}\alpha_1\\ \alpha_2\end{bmatrix} \tag{1.10}$$

satisfies, uniformly in $\varepsilon \in (0,1]$ and $t > 0$,

$$\Psi_t(x) = \frac{\lambda_1}{\sqrt{\varepsilon}} \cdot \exp\left(-\frac{|x-y_t|^2}{2\varepsilon}\right)\begin{bmatrix}e^{-i\theta_t/2}\\ -e^{i\theta_t/2}\end{bmatrix} + \mathcal{O}_{L^2}\left(\varepsilon^{1/2}\langle t\rangle\right) + \mathcal{O}_{L^\infty}\left(\varepsilon^{-1/4}t^{-1/2}\right). \tag{1.11}$$

When starting with the two-spinor $[\alpha_1, \alpha_2]^\top = [e^{-i\theta_0/2}, e^{i\theta_0/2}]^\top$, that is, the orthogonal spinor to that in (1.3), we have $\lambda_1 = 0$. Hence (1.11) takes the form

$$\Psi_t(x) = \mathcal{O}_{L^\infty}\left(\varepsilon^{-1/4}t^{-1/2}\right) + \mathcal{O}_{L^2}\left(\varepsilon^{1/2}\right). \tag{1.12}$$

According to this conjecture, while Ψ_0 has an $\varepsilon^{-1/2}$-peaked profile, for any $1 \le t \le 2$ (say), the solution Ψ_t is, up to a small remainder in L^2, uniformly bounded as $\varepsilon \to 0$. This means that Ψ_t loses its initial wavepacket structure. Data carried by the spinor orthogonal to (1.3) appear to disperse along the edge instead of propagating in the opposite direction. This contrasts with the standard behavior of wavepackets in semiclassical systems; see (1.8).

The general case $\lambda_1 \neq 0$ is the linear superposition of $\lambda_1 = 0$ with Theorem 1. According to (1.12), the dynamical edge state emerges as the dominant component of Ψ_t in L^∞ as t grows. We refer to Conjecture 2 for a more general version of Conjecture 1. We mention that (1.11) has been proved for times $t \in (0, t_0]$, where t_0 is a small parameter depending on κ; see [16, 4]. The proofs rely on microlocal reductions and a WKB analysis. The associated eikonal equation is analyzed in small time only, which explains the restriction $t \in (0, t_0]$. The conjecture for large times remains open.

1.6. Organization of the paper. We organize the paper as follows:

- In section 2 we review edge state theory for Dirac operators with straight domain walls, i.e., $\kappa(x) = a \cdot x$ in (1.1).

- In section 3 we derive the analogues of edge states for weakly curved interface. Specifically, we construct a infinite-dimensional family of solutions to $(\varepsilon D_t + H)\Psi_t = 0$ that propagates along the topological interface Γ for times up to $\varepsilon^{-1/2}$. The key ingredient is a local approximation of H by Dirac operators with straight interfaces.
- In section 4 we investigate, under a geometric condition of κ, how the curvature of Γ affects the propagation of wavepackets.

Notations.

- We use $\sigma_1, \sigma_2, \sigma_3$ for the standard Pauli matrices
$$\sigma_1 = \begin{bmatrix} 0 & 1 \\ 1 & 0 \end{bmatrix}, \quad \sigma_2 = \begin{bmatrix} 0 & -i \\ i & 0 \end{bmatrix}, \quad \sigma_3 = \begin{bmatrix} 1 & 0 \\ 0 & -1 \end{bmatrix}.$$
- A smooth function f on $\mathbb{R}^2$ belongs to $C_b^\infty(\mathbb{R}^2)$ if it is uniformly bounded, together with its derivatives at all order.
- A function $f \in C_b^\infty(\mathbb{R}^2)$ belongs to $\mathcal{S}(\mathbb{R}^2)$ if $x^\alpha \partial_x^\beta f$ is uniformly bounded for any α, β. We provide $\mathcal{S}(\mathbb{R}^2)$ with the family of seminorms $|x^\alpha \partial_x^\beta f|_{L^\infty}$.
- The operators D_{x_j} and D_t are defined by $D_{x_j} = -i\partial_{x_j}$ and $D_t = -i\partial_t$.
- We use the Japanese bracket notation $\langle x \rangle = \sqrt{1 + |x|^2}$.
- We denote by $\ker_{\mathcal{V}}(A)$ the kernel of a linear operator A acting on a vector space $\mathcal{V}$.
- If $v \in \mathbb{R}^2$, $v^\perp$ is the counterclockwise $\pi/2$-rotation of v.
- $\langle u, v \rangle_{L^2} = \int_{\mathbb{R}^2} \overline{u} v$.
- For f in a normed vector space $\mathcal{X}$, we write $f = \mathcal{O}_{\mathcal{X}}(\varepsilon)$ if $|f|_{\mathcal{X}} \leq C\varepsilon$ for some constant $C > 0$ independent of ε.
- Given $\alpha \in \mathbb{C}^2$, $\alpha^\perp = -i\sigma_2\alpha$ is the $\pi/2$-rotation of α.
- y_t is the solution to the ODE (1.2) with initial data $y_0 \in \Gamma$; θ_t is the angle between the y-axis and $\nabla\kappa(y_t)$; and $r_t = |\nabla\kappa(y_t)|$. See Figure 1.

2. Edge states and dynamics for straight interfaces. We review here the simplest example of domain wall κ: we write

$$\kappa(x) = \kappa_{\theta,r}(x) = -r\sin(\theta)x_1 + r\cos(\theta)x_2 = r\begin{bmatrix} -\sin(\theta) \\ \cos(\theta) \end{bmatrix} \cdot x$$

with $\theta \in \mathbb{R}$, $r > 0$. We note that $\nabla\kappa$ is constant; in particular, $\nabla\kappa \in C_b^\infty(\mathbb{R}^2)$. The interface $\kappa_{\theta,r}^{-1}(0) = \mathbb{R}v_\theta$ is a straight line, directed by the vector $v_\theta = -[\cos(\theta), \sin(\theta)]^\top$; see Figure 7. The Hamiltonian is then

$$H_{\theta,r} = \begin{bmatrix} \kappa_{\theta,r}(x) & \varepsilon D_{x_1} - i\varepsilon D_{x_2} \\ \varepsilon D_{x_1} + i\varepsilon D_{x_2} & -\kappa_{\theta,r}(x) \end{bmatrix}. \tag{2.1}$$

It admits edge states: there exist eigenfunctions of the operator $H_{\theta,r}$ that are localized and harmonic along $\mathbb{R}v_\theta$ (see (2.5) below). Here we review their explicit expression and their dynamical properties.

2.1. Conjugation properties. We first show that the Hamiltonians $H_{\theta,r}$ and $H_{0,r}$ are conjugated by a change of frame and gauge. For this purpose, we introduce the operator

$$\mathcal{U}_\theta f(x) = U_\theta f(R_\theta x), \quad R_\theta = \begin{bmatrix} \cos(\theta) & \sin(\theta) \\ -\sin(\theta) & \cos(\theta) \end{bmatrix}; \quad U_\theta = \begin{bmatrix} e^{-i\theta/2} & 0 \\ 0 & e^{i\theta/2} \end{bmatrix}. \tag{2.2}$$

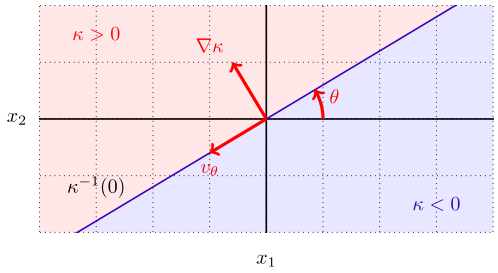

FIG. 7. *Currents propagate along* Γ *at speed* v_θ *given by the counterclockwise rotation of* $\nabla\kappa$.

LEMMA 2.1. *The Hamiltonian* (2.1) *is unitarily equivalent to the Hamiltonian* $H_{0,r}$ *with*

$$\mathcal{U}_\theta^{-1} H_{\theta,r} \mathcal{U}_\theta = H_{0,r}.$$

Proof. Let $\mathcal{R}_\theta$ be the pullback operator by R_θ: $\mathcal{R}_\theta f(x) = f(R_\theta x)$. We note that $\kappa_{\theta,r}(x) = r \cdot R_\theta^\top e_2 \cdot x = r(R_\theta x)_2$. Thus $\mathcal{R}_\theta^{-1}\kappa_{\theta,r}\mathcal{R}_\theta = rx_2$. We now use $\mathcal{R}_\theta^{-1} D_x \mathcal{R}_\theta = R_\theta^\top D_x$ to compute partial derivatives involved in $H_{\theta,r}$:

$$\mathcal{R}_\theta^{-1}(D_{x_1} + iD_{x_2})\mathcal{R}_\theta = \begin{bmatrix}1\\ i\end{bmatrix} \cdot R_\theta^\top D_x = R_\theta \begin{bmatrix}1\\ i\end{bmatrix} \cdot D_x = \begin{bmatrix}e^{i\theta}\\ ie^{i\theta}\end{bmatrix} \cdot D_x = e^{i\theta}(D_{x_1} + iD_{x_2}).$$

The adjoint identity is

$$\mathcal{R}_\theta^{-1}(D_{x_1} - iD_{x_2})\mathcal{R}_\theta = e^{-i\theta}(D_{x_1} - iD_{x_2}).$$

Grouping these identities, we obtain

$$\begin{aligned}\mathcal{R}_\theta^{-1} H_{\theta,r} \mathcal{R}_\theta &= \begin{bmatrix} rx_2 & e^{-i\theta}\varepsilon(D_{x_1} - iD_{x_2}) \\ e^{i\theta}\varepsilon(D_{x_1} + iD_{x_2}) & -rx_2 \end{bmatrix} \\ &= s_1 \varepsilon D_{x_1} + s_2 \varepsilon D_{x_2} + s_3 r x_2,\end{aligned}$$

where, s_1, s_2, s_3 are 2×2 Hermitian matrices given by

$$s_1 = \begin{bmatrix} 0 & e^{-i\theta} \\ e^{i\theta} & 0 \end{bmatrix}, \quad s_2 = \begin{bmatrix} 0 & -ie^{-i\theta} \\ ie^{i\theta} & 0 \end{bmatrix}, \quad s_3 = \begin{bmatrix} 1 & 0 \\ 0 & -1 \end{bmatrix} = \sigma_3.$$

An explicit calculation shows that $U_\theta^{-1} s_j U_\theta = \sigma_j$. We conclude that

$$\mathcal{U}_\theta^{-1} H_{\theta,r}\, \mathcal{U}_\theta = \sigma_1 \varepsilon D_{x_1} + \sigma_2 \varepsilon D_{x_2} + \sigma_3 x_2 = H_{0,r}. \tag{2.3}$$

This completes the proof. ∎

Remark 1. The relation (2.2) allows us to calculate the conductivity of $H_{\theta,r}$ in the direction of v_θ; see (1.5): it is equal to 1. Indeed, the conductivity of $H_{0,r}$ (counted positively in the direction of $e_2^\perp = -e_1$) is equal to 1 [2]. We claim then that, for f, g two scalar functions,

$$1 = \mathrm{Tr}_{L^2}\Big(\big[H_{0,r}, f(-x_1)\big] g'(H_{0,r})\Big) = \mathrm{Tr}_{L^2}\Big(\big[H_{\theta,r}, f(v_\theta \cdot x)\big] g'(H_{\theta,r})\Big). \tag{2.4}$$

Indeed, we have

$$[H_0, f(-x_1)] = \mathcal{U}_\theta^{-1}\left[H_{\theta,r}, \mathcal{U}_\theta f(-x_1) \mathcal{U}_\theta^{-1}\right] \mathcal{U}_\theta,$$

and, since f is scalar,

$$\mathcal{U}_\theta f(-x_1)\mathcal{U}_\theta^{-1} = \mathcal{R}_\theta f(-x_1)\mathcal{R}_\theta^{-1}\ U_\theta^{-1}U_\theta = \mathcal{R}_\theta f(-x_1)\mathcal{R}_\theta^{-1} = f(-v_\theta\cdot x).$$

As a consequence of these computations and in view of the relation $g'(H_{\theta,r}) = \mathcal{U}_\theta g'(H_{0,r})\mathcal{U}_\theta^{-1}$ and of the invariance of the trace under conjugation, we obtain (2.4).

The Hamiltonian $H_{0,r}$ admits edge states: for any $\xi\in\mathbb{R}$, if

$$F_{0,r}(\xi,x) = \exp\left(\frac{i\xi x_1}{\varepsilon} - \frac{rx_2^2}{2\varepsilon}\right)\begin{bmatrix}1\\-1\end{bmatrix},$$

then $F_{0,r}(\xi,\cdot)$ is a plane wave in x_1, i.e., along the interface; decays transversely along the interface, i.e., in x_2; and satisfies the stationary Dirac equation $(H_{0,r}-\xi)$ $F_{0,r}(\xi,\cdot)=0$. From Lemma 2.1 we deduce that $H_{\theta,r}$ also admits edge states: the function

$$F_{\theta,r}(\xi,x) = \mathcal{U}_\theta F_{0,r}(\xi,x) = \exp\left(\frac{i\xi(R_\theta x)_1}{\varepsilon} - \frac{r(R_\theta x)_2^2}{2\varepsilon}\right)\begin{bmatrix}e^{-i\theta/2}\\-e^{i\theta/2}\end{bmatrix} \tag{2.5}$$

satisfies $(H_{\theta,r}-\xi)F_{\theta,r}(\xi,\cdot)=0$.

2.2. Dynamics of edge states. We review here how edge states give rise to an infinite-dimensional family of ballistic waves for Dirac operators with linear domain walls.

PROPOSITION 2.2. *For any $f\in\mathcal{S}(\mathbb{R})$, the function*

$$\psi_t(x) = \varepsilon^{-1/2}\cdot f\big(t+(R_\theta x)_1\big)\cdot\exp\left(-\frac{r(R_\theta x)_2^2}{2\varepsilon}\right)\begin{bmatrix}e^{-i\theta/2}\\-e^{i\theta/2}\end{bmatrix} \tag{2.6}$$

solves the equation $(\varepsilon D_t + H_{\theta,r})\psi_t = 0$.

The functions (2.6) are the ballistic waves generated by edge states; they propagate along the interface $\mathbb{R}v_\theta$ and decay rapidly along $\mathbb{R}v_\theta^\perp$. Our scaling casts (2.6) as wavepackets:

$$\psi_t(x) = \varepsilon^{-1/2}\cdot a\left(\frac{x-y_t}{\sqrt{\varepsilon}}\right),\quad a(y) = e^{-\frac{r}{2}(R_\theta y)_2^2} f\big(\sqrt{\varepsilon}(R_\theta y)_1\big)\begin{bmatrix}e^{-i\theta/2}\\-e^{i\theta/2}\end{bmatrix},\quad y_t = tv_\theta, \tag{2.7}$$

with a having a full asymptotic expansion in powers of $\sqrt{\varepsilon}$. This connection will be the basis of our analysis in the context of curved interfaces.

Proof of Proposition 2.2. The ε-scaled Fourier transform in time allows us to take advantage of the relation $(H_{\theta,r}-\xi)F_{\theta,r}(\xi,\cdot)=0$ (existence of edge states) to construct a solution to the equation $(\varepsilon D_t + H_{\theta,r})\psi_t = 0$. Let $g\in\mathcal{S}(\mathbb{R})$ such that

$$g(\xi) = \frac{1}{2\pi\varepsilon}\int_{\mathbb{R}} e^{\frac{i}{\varepsilon}t\xi} f(t)dt.$$

We introduce

$$\psi_t(x) = \varepsilon^{-1/2}\int_{\mathbb{R}} e^{-\frac{i}{\varepsilon}t\xi} g(\xi)F_{\theta,r}(\xi,x)d\xi. \tag{2.8}$$

Since $(H_{\theta,r}-\xi)F_{\theta,r}(\xi,\cdot)=0$, we deduce that

$$\begin{aligned}\varepsilon D_t\psi_t(x) &= -\varepsilon^{-1/2}\int_{\mathbb{R}} \xi e^{-\frac{i}{\varepsilon}t\xi} g(\xi)F_{\theta,r}(\xi,x)d\xi \\ &= -\varepsilon^{-1/2}\int_{\mathbb{R}} e^{-\frac{i}{\varepsilon}t\xi} g(\xi)H_{\theta,r}F_{\theta,r}(\xi,x)d\xi = -H_{\theta,r}\psi_t(x),\end{aligned}$$

where we have used that $H_{\theta,r}$ does not depend on ξ. This proves that (2.8) is a solution to $(\varepsilon D_t + H_{\theta,r})\psi_t = 0$. Plugging the formula (2.5) for $F_{\theta,r}$ in (2.8), we obtain

$$\begin{aligned}\psi_t(x) &= \varepsilon^{-1/2}\int_{\mathbb{R}} e^{-\frac{i}{\varepsilon}(t+(R_\theta x)_1)\xi} g(\xi)d\xi \cdot \exp\left(-\frac{r(R_\theta x)_2^2}{2\varepsilon}\right)\begin{bmatrix} e^{-i\theta/2} \\ -e^{i\theta/2}\end{bmatrix} \\ &= \varepsilon^{-1/2} f\big(t+(R_\theta x)_1\big)\exp\left(-\frac{r(R_\theta x)_2^2}{2\varepsilon}\right)\begin{bmatrix} e^{-i\theta/2} \\ -e^{i\theta/2}\end{bmatrix},\end{aligned}$$

by definition of g as the inverse (semiclassical) Fourier transform of f. ∎

3. Dynamical analogues of edge states along curved interfaces. We now consider nonlinear domain walls, opening the possibility for curved topological interfaces. We relax (1.2) to a global transversality condition

$$\inf\big\{\big|\nabla\kappa(y)\big|:\ \kappa(y)=0\big\} > 0. \tag{3.1}$$

We recall that all derivatives of κ are uniformly bounded: $\nabla\kappa \in C_b^\infty(\mathbb{R}^2)$. We plan to produce a dynamical analogue of edge states, a solution to

$$(\varepsilon D_t + H)\psi = 0, \qquad H = \begin{bmatrix} \kappa(x) & \varepsilon D_{x_1} - i\varepsilon D_{x_2} \\ \varepsilon D_{x_1} + i\varepsilon D_{x_2} & -\kappa(x)\end{bmatrix},$$

that propagates for long time along the topological interface $\Gamma = \kappa^{-1}(0)$.

The equation (2.7) motivates the ansatz

$$\psi(t,x) = \varepsilon^{-1/2} a\left(t, \frac{x-y_t}{\sqrt{\varepsilon}}\right), \qquad \text{where}$$

- $a \in \mathcal{S}(\mathbb{R}^2,\mathbb{C}^2)$ has a full expansion in powers of $\varepsilon^{1/2}$;
- $y_0 \in \Gamma$ and $y_t \in \Gamma$ is the solution of the ODE

$$\dot{y_t} = v(y_t), \qquad v(y) = \frac{\nabla\kappa(y)^\perp}{|\nabla\kappa(y)|}, \qquad w^\perp = \begin{bmatrix} 0 & -1 \\ 1 & 0\end{bmatrix} w.$$

The vector $v(y)$ is the local analogue to v_θ: at each point $y \in \Gamma$, it is the unit tangent vector to Γ obtained by rotating counterclockwise $\nabla\kappa(y)$. Since $\kappa(y_0)=0$, $y_t \in \Gamma$ for any t,

$$\frac{d\kappa(y_t)}{dt} = \dot{y_t}\cdot\nabla\kappa(y_t) = v(y_t)\cdot\nabla\kappa(y_t) = 0.$$

Let θ_t and r_t be such that

$$\nabla\kappa(y_t) = r_t\begin{bmatrix} -\sin(\theta_t) \\ \cos(\theta_t)\end{bmatrix} \quad \text{so that} \quad v(y_t) = -\begin{bmatrix}\cos(\theta_t) \\ \sin(\theta_t)\end{bmatrix}; \tag{3.2}$$

see Figure 1. With these notations in place, we define $\mathcal{K}_t : \mathcal{S}(\mathbb{R}) \to \mathcal{S}(\mathbb{R}^2,\mathbb{C}^2)$ by

$$\mathcal{K}_t f(x) = r_t^{1/4} f\big((R_{\theta_t}x)_1\big) e^{-\frac{r_t}{2}(R_{\theta_t}x)_2^2}\begin{bmatrix} e^{-i\theta_t/2} \\ -e^{i\theta_t/2}\end{bmatrix}, \qquad f \in \mathcal{S}(\mathbb{R}). \tag{3.3}$$

THEOREM 2. *Let $\kappa \in C^\infty(\mathbb{R}^2)$ satisfy (3.1) with $\nabla\kappa \in C_b^\infty(\mathbb{R}^2)$ and y_t, θ_t as above. Let $f_0 \in \mathcal{S}(\mathbb{R})$ and ψ_t be the solution to $(\varepsilon D_t + H)\psi_t = 0$ with*

$$\psi_0(x) = \frac{1}{\sqrt{\varepsilon}} \cdot \mathcal{K}_0 f_0\left(\frac{x - y_0}{\sqrt{\varepsilon}}\right). \tag{3.4}$$

Then, uniformly for $\varepsilon \in (0,1]$ and $t > 0$,

$$\psi_t(x) = \frac{1}{\sqrt{\varepsilon}} \cdot \mathcal{K}_t f\left(\frac{x - y_t}{\sqrt{\varepsilon}}\right) + \mathcal{O}_{L^2}\left(\varepsilon^{1/2}\langle t\rangle\right). \tag{3.5}$$

Theorem 2 constructs a solution to $(\varepsilon D_t + H)\psi_t = 0$, propagating dispersion-free along y_t, for times $t \ll \varepsilon^{-1/2}$. Under geometric conditions on κ, we can extend this time of validity; see Theorem 4. These two results focus on maximizing the lifespan of approximate solutions. We can instead focus on improving their accuracy: see Theorem 3 for solutions up to $O(\varepsilon^n)$ for every n but fixed lifetime.

When r_t is not constant—corresponding to (3.1) holding instead of (1.2)—the state in (3.5) is coherent in a relaxed sense: there may be lateral spreading at scale r_t (which remains bounded above and below by our assumptions on κ). See the expression (3.3) for $\mathcal{K}_t f$ and Figure 5 for a numerical illustration.

The initial data (3.4) are quite specific: the rescaled amplitude $\mathcal{K}_0 f$ is in the range of $\mathcal{K}_0$. To obtain a full picture of evolution of states initially microlocalized along $\mathcal{C}$, we need to understand how orthogonal initial data propagate:

$$\psi_0(x) = \frac{1}{\sqrt{\varepsilon}} \cdot \mathcal{K}_0 f\left(\frac{x - y_0}{\sqrt{\varepsilon}}\right)^{\perp}.$$

This suggests a refinement of Conjecture 1. Let $\Pi : \mathcal{S}(\mathbb{R}^2, \mathbb{C}^2) \to \mathcal{S}(\mathbb{R}^2, \mathbb{C}^2)$ be the orthogonal projection on the range of $\mathcal{K}_0$. We observe that $\mathcal{K}_0$ is an isomorphism to its range; therefore, for any $a \in \mathcal{S}(\mathbb{R}^2, \mathbb{C}^2)$, there exists a unique $f \in \mathcal{S}(\mathbb{R})$ such that $\Pi a = \mathcal{K}_0 f$.

CONJECTURE 2. *Let $a \in \mathcal{S}(\mathbb{R}^2, \mathbb{C}^2)$, $f \in \mathcal{S}(\mathbb{R})$ such that $\Pi a = \mathcal{K}_0 f$, and let ϕ_t be the solution to $(\varepsilon D_t + H)\phi_t = 0$ with initial data*

$$\phi_0(x) = \frac{1}{\sqrt{\varepsilon}} \cdot a\left(\frac{x - y_0}{\sqrt{\varepsilon}}\right).$$

Then, uniformly in $\varepsilon \in (0,1]$, $t > 0$,

$$\phi_t(x) = \frac{1}{\sqrt{\varepsilon}} \cdot \mathcal{K}_t f\left(\frac{x - y_t}{\sqrt{\varepsilon}}\right) + \mathcal{O}_{L^2}\left(\varepsilon^{1/2}\langle t\rangle\right) + \mathcal{O}_{L^\infty}\left(\varepsilon^{-1/4} t^{-1/2}\right).$$

According to Conjecture 2, any function localized (in a semiclassical sense) near $(y_0, 0)$ splits in propagating and dispersive parts, with an edge state analogue emerging dynamically. See Figure 4 for a numerical confirmation.

3.1. Structure of proof of Theorem 2. We will prove Theorem 2 by establishing the following statements:

1. Approximate solutions of the Dirac equation solve a hierarchy of transport equations; see Lemma 3.1.
2. The leading-order transport operator has explicit kernel and a spectral gap away from its kernel; see section 3.3.
3. Solutions to the hierarchy of transport equations exist; see sections 3.4–3.5.

4. Approximate and exact solutions to the Dirac equation are nearly equal; see section 3.6.

We will use the notation

$$W[a]_{y_t}(x) = \frac{1}{\sqrt{\varepsilon}} \cdot a\left(\frac{x - y_t}{\sqrt{\varepsilon}}\right)$$

for $a \in \mathcal{S}(\mathbb{R}^2, \mathbb{C}^2)$ possibly depending on t and ε.

We also introduce the operators T_j acting on $\mathcal{S}(\mathbb{R}^2, \mathbb{C}^2)$, defined by

$$T_0 = -\dot{y_t} \cdot D_x + \begin{bmatrix} \nabla\kappa(y_t) \cdot x & D_{x_1} - iD_{x_2} \\ D_{x_1} + iD_{x_2} & -\nabla\kappa(y_t) \cdot x \end{bmatrix}, \tag{3.6}$$

$$T_1 = D_t + \left(\sum_{|\alpha|=2} \frac{1}{\alpha!} \partial^\alpha \kappa(y_t) x^\alpha\right) \sigma_3, \tag{3.7}$$

$$T_j = \left(\sum_{|\alpha|=j+1} \frac{1}{\alpha!} \partial^\alpha \kappa(y_t) x^\alpha\right) \sigma_3, \ j \geq 2. \tag{3.8}$$

3.2. Formal approximate solutions via transport equations. We start with the following lemma: solving the hierarchy of transport equations

$$T_0 a_0 = 0, \quad T_0 a_1 + T_1 a_0 = 0, \quad \ldots, \quad \sum_{\ell=0}^{j} T_{j-\ell} a_\ell = 0, \quad j \in [0, m] \tag{3.9}$$

produces approximate solutions to the Dirac equation.

LEMMA 3.1. *For any $m \in \mathbb{N}$ there exists $C > 0$ such that if a_0, a_1, …, $a_m \in \mathcal{S}(\mathbb{R}^2, \mathbb{C}^2)$ are solutions of* (3.9) *and $a^{(m)} = \sum_{\ell=0}^{m} \varepsilon^{\ell/2} a_\ell$, then, for all $\varepsilon \in (0, 1]$,*

$$\left\| (\varepsilon D_t + H) W\left[a^{(m)}\right]_{y_t} \right\|_{L^2} \leq C\varepsilon^{\frac{m+2}{2}} \left(\|D_t a_m\|_{L^2} + \sum_{k=0}^{m} \left\| \langle x \rangle^{m+2} a_k \right\|_{L^2} \right).$$

Proof of Lemma 3.1. **1.** Fix $m \in \mathbb{N}$. We observe that, for $a \in \mathcal{S}(\mathbb{R}^2, \mathbb{C}^2)$,

$$\varepsilon \partial_{x_j} W[a]_{y_t} = W[\sqrt{\varepsilon}\, \partial_{x_j} a]_{y_t}, \ \varepsilon D_t W[a]_{y_t} = W[-\sqrt{\varepsilon}\, \dot{y_t} \cdot D_x a + \varepsilon D_t a]_{y_t}. \tag{3.10}$$

We now write the Taylor–Lagrange identity with the following integral remainder (note that $\kappa(y_t) = 0$):

$$\kappa(x) = \left(\sum_{|\alpha|=1}^{m+1} \frac{1}{\alpha!} \partial^\alpha \kappa(y_t)(x - y_t)^\alpha\right) + r_m(x - y_t), \quad \text{with}$$

$$r_m(x) = \frac{1}{(m+1)!} \sum_{|\alpha|=m+2} x^\alpha \int_0^1 (1 - s)^{m+1} \partial^\alpha \kappa\big(y_t + sx\big) ds.$$

We observe $(x-y_t)^\alpha W[a]_{y_t}(x) = \varepsilon^{\frac{|\alpha|}{2}} W[x^\alpha a]$. Therefore, we deduce

(3.11)
$$\kappa(x)W[a]_{y_t}(x) = W\left[\left(\sum_{|\alpha|=1}^{m+1}\frac{\varepsilon^{|\alpha|/2}}{\alpha!}\partial^\alpha\kappa(y_t)x^\alpha + \varepsilon^{\frac{m+2}{2}}R_m(x)\right)a\right]_{y_t}(x), \quad \text{with}$$
$$R_m(x) = \varepsilon^{-\frac{m+2}{2}} r_m(\varepsilon^{1/2}x)$$
$$= \frac{1}{(m+1)!}\sum_{|\alpha|=m+2} x^\alpha \int_0^1 (1-s)^{m+1}\partial^\alpha\kappa\big(y_t + s\varepsilon^{1/2}x\big)ds.$$

Since $\nabla\kappa \in C_b^\infty(\mathbb{R}^2,\mathbb{R}^2)$, we have $|r_m(x)| \le C|x|^{m+2}$; therefore $R_m(x) \le C|x|^{m+2}$ for all $\varepsilon \in (0,1]$. From the relations (3.10)–(3.11) and the definition (3.8) of the operators T_j,

$$(\varepsilon D_t + H)W[a]_{y_t} = W\left[\left(\sum_{j=0}^{m}\varepsilon^{\frac{j+1}{2}}T_j + \varepsilon^{\frac{m+2}{2}}R_m\right)a\right]_{y_t}.$$

In particular, using that $W[a]_{y_t}$ and a have the same L^2-norm,

$$\big\|(\varepsilon D_t + H)W[a]_{y_t}\big\|_{L^2} = \left\|\left(\sum_{j=0}^{m}\varepsilon^{\frac{j+1}{2}}T_j + \varepsilon^{\frac{m+2}{2}}R_m\right)a\right\|_{L^2}. \tag{3.12}$$

2. Assume now that a_j solves (3.9), and plug $a^{(m)} = \sum_{k=0}^m \varepsilon^{k/2}a_k$ for the amplitude in (3.12). Then we obtain

$$\big\|(\varepsilon D_t + H)W[a^{(m)}]_{y_t}\big\|_{L^2} = \left\|\sum_{\substack{j,k=0\\ j+k\ge m+1}}^{m}\varepsilon^{\frac{j+k+1}{2}}T_j a_k + \sum_{k=0}^{m}\varepsilon^{\frac{m+2+k}{2}}R_m a_k\right\|_{L^2}.$$

Note that the conditions $j,k\le m$ and $j+k\ge m+1$ yield $j,k\neq 0$. Therefore, we have

$$\big\|(\varepsilon D_t + H)W[a^{(m)}]_{y_t}\big\|_{L^2} \le \sum_{\substack{j,k=1\\ j+k\ge m+1}}^{m}\varepsilon^{\frac{j+k+1}{2}}\big\|T_j a_k\big\|_{L^2} + \sum_{k=0}^{m}\varepsilon^{\frac{m+2+k}{2}}\big\|R_m a_k\big\|_{L^2}.$$

In the second line we used the first sum starts at $j,k=1$, since $j+k\ge m+1$ and $j,k\le m$.

In view of (3.7) and (3.8), we obtain the existence of $C>0$ such that, for all $a\in\mathcal{S}(\mathbb{R}^2,\mathbb{C}^2)$,

$$\|T_1 a\|_{L^2} \le \|D_t a\|_{L^2} + \sum_{|\alpha|=2}\frac{1}{\alpha!}|\partial^\alpha\kappa(y_t)|\|x^\alpha a\|_{L^2} \le \|D_t a\|_{L^2} + C\|\langle x\rangle^2 a\|_{L^2},$$

and for $j\in\mathbb{N}$,

$$\|T_j a\|_{L^2} \le \sum_{|\alpha|=j+1}\frac{1}{\alpha!}|\partial^\alpha\kappa(y_t)|\|x^\alpha a\|_{L^2} \le C\|\langle x\rangle^{j+1}a\|_{L^2}.$$

Similarly, by modifying C if necessary,

$$\|R_m a\|_{L^2} \le C\|\langle x\rangle^{m+2} a\|_{L^2}.$$

In these estimates, we have used the boundedness of the derivatives of κ. We deduce that $\|(\varepsilon D_t + H)W[a^{(m)}]_{y_t}\|_{L^2}$ is bounded, up to a multiplicative constant, by

$$\varepsilon^{\frac{m+2}{2}}\|D_t a_m\|_{L^2} + \varepsilon^{\frac{m+2}{2}}\|\langle x\rangle^2 a_m\|_{L^2} + \sum_{\substack{j,k=1\\ j+k\ge m+1;\, j\ge 2}}^{m} \varepsilon^{\frac{j+k+1}{2}}\|\langle x\rangle^{j+1} a_k\|_{L^2} + \sum_{k=0}^{m} \varepsilon^{\frac{m+2+k}{2}}\|\langle x\rangle^{m+2} a_k\|_{L^2},$$

whence by

$$\varepsilon^{\frac{m+2}{2}}\|D_t a_m\|_{L^2} + \sum_{\substack{j,k=1\\ j+k\ge m+1}}^{m} \varepsilon^{\frac{j+k+1}{2}}\left\|\langle x\rangle^{m+2} a_k\right\|_{L^2} + \sum_{k=0}^{m}\varepsilon^{\frac{m+2+k}{2}}\left\|\langle x\rangle^{m+2} a_k\right\|_{L^2}.$$

Noting that $j + k + 1 \ge m + 2$ in the first sum, we conclude that, for any t,

$$\left\|(\varepsilon D_t + H)W[a^{(m)}]_{y_t}\right\|_{L^2} \le C\varepsilon^{\frac{m+2}{2}}\left(\|D_t a_m\|_{L^2} + \sum_{k=0}^{m}\left\|\langle x\rangle^{m+2} a_k\right\|_{L^2}\right).$$

This completes the proof. ∎

We will show in the following how to construct solutions a_j to the hierarchy (3.9) and then bound their derivatives and moments. Together with Lemma 3.1 this will give a rigorous construction of approximate solutions to the Dirac equation.

3.3. Spectral analysis of leading-order transport operator. The dominant equation of the hierarchy (3.9) is $T_0 a_0 = 0$, where T_0 is defined in (3.6); the other equations are

$$T_0 a_j = -\sum_{\ell=0}^{j-1} T_{j-\ell} a_\ell, \quad 1 \le j \le m.$$

Solving these equations amounts to (i) find $\ker(T_0)$ and (ii) establish a stability estimate (here, a spectral gap) for T_0^{-1} away from $\ker(T_0)$. Below we write $T_0 = L_{\theta_t, r_t}$, where

$$L_{\theta,r} = \begin{bmatrix}\cos(\theta)\\ \sin(\theta)\end{bmatrix} D_x + \begin{bmatrix} r\kappa_{\theta,r}(x) & D_{x_1} - iD_{x_2}\\ D_{x_1} + iD_{x_2} & -r\kappa_{\theta,r}(x)\end{bmatrix} = \begin{bmatrix}\cos(\theta)\\ \sin(\theta)\end{bmatrix} D_x + H_{r,\theta}. \tag{3.13}$$

We now focus on the analysis of $L_{\theta,r}$ on $\mathcal{S}(\mathbb{R}^2, \mathbb{C}^2)$. We first compute its kernel (Lemma 3.2) and prove it is one to one on the orthogonal complement (Lemma 3.3).

LEMMA 3.2. *For every $r > 0$ and $\theta \in \mathbb{R}$, the nullspace of $L_{\theta,r} : \mathcal{S}(\mathbb{R}^2, \mathbb{C}^2) \to \mathcal{S}(\mathbb{R}^2, \mathbb{C}^2)$ is*

$$\ker_{\mathcal{S}(\mathbb{R}^2)}(L_{\theta,r}) = \left\{ f\big((R_\theta x)_1\big) e^{-\frac{r(R_\theta x)_2^2}{2}} \begin{bmatrix} e^{-i\theta/2}\\ -e^{i\theta/2}\end{bmatrix},\ f \in \mathcal{S}(\mathbb{R})\right\}. \tag{3.14}$$

Proof. As in (2.3), $\mathcal{U}_\theta^{-1} L_{\theta,r} \mathcal{U}_\theta = L_{0,r}$, with $\mathcal{U}_\theta = \mathcal{R}_\theta U_\theta$. Indeed, $U_\theta^{-1}\mathcal{R}_\theta^{-1} H_\theta \mathcal{R}_\theta U_\theta = H_0$ and

$$\mathcal{U}_\theta^{-1} \begin{bmatrix} \cos(\theta) \\ \sin(\theta) \end{bmatrix} \cdot D_x \mathcal{U}_\theta = R_\theta^\top e_1 \cdot R_\theta^\top D_x = D_{x_1}.$$

Moreover, if $S_r f(x) = f(\sqrt{r}x)$, then we have

$$S_r^{-1} H_{0,r} S_r = \sqrt{r} H_{0,1}.$$

Hence, $H_{\theta,r}$ and $H_{0,1}$ are conjugated (up to multiplication by $\sqrt{r}$). The identity (3.13) implies that the same holds for $L_{\theta,r}$ and $L_{0,1}$:

$$S_r^{-1} \mathcal{U}_\theta^{-1} L_{\theta,r} \mathcal{U}_\theta S_r = \sqrt{r} L_{0,1}. \tag{3.15}$$

Thus, to find the kernel of $L_{\theta,r}$, it suffices to find that of $L_{0,1}$. We have

$$L_{0,1} = \begin{bmatrix} D_{x_1} + x_2 & D_{x_1} - iD_{x_2} \\ D_{x_1} + iD_{x_2} & D_{x_1} - x_2 \end{bmatrix} = \begin{bmatrix} 1 & 1 \\ 1 & 1 \end{bmatrix} D_{x_1} + \begin{bmatrix} x_2 & -iD_{x_2} \\ iD_{x_2} & -x_2 \end{bmatrix}.$$

We claim that

$$\ker_{\mathcal{S}(\mathbb{R}^2)}(L_{0,1}) = \left\{ f(x_1) e^{-\frac{x_2^2}{2}} \begin{bmatrix} 1 \\ -1 \end{bmatrix} : \ f \in \mathcal{S}(\mathbb{R}) \right\}. \tag{3.16}$$

The right inclusion follows from a computation. To prove the left inclusion, we pick u such that $L_{0,1} u = 0$. We take the Fourier transform in x_1: this gives $L_{0,1}(\xi)\widehat{u} = 0$, where

$$L_{0,1}(\xi) = \xi \begin{bmatrix} 1 & 1 \\ 1 & 1 \end{bmatrix} + \begin{bmatrix} x_2 & -iD_{x_2} \\ iD_{x_2} & -x_2 \end{bmatrix}.$$

We fix ξ. The operator $L_{0,1}(\xi)$ is a linear differential operator; hence the space of decaying solutions to $L_{0,1}(\xi)v = 0$ is at most one-dimensional. Indeed, if v_1, v_2 are such functions, then their Wronskian is constant, and they decay. Thus their Wronskian vanishes; this implies that v_1, v_2 are linearly dependent. We then observe that

$$L_{0,1}(\xi) e^{-\frac{x_2^2}{2}} \begin{bmatrix} 1 \\ -1 \end{bmatrix} = 0.$$

This shows that the kernel of $L_{0,1}(\xi)$ is one-dimensional. Superposing over ξ yields (3.16). Applying the equivalence between $L_{0,1}$ and $L_{\theta,r}$, we conclude that the kernel of $L_{\theta,r}$ is precisely made of functions

$$S_r \mathcal{R}_\theta U_\theta \left(f(x_1) e^{-\frac{x_2^2}{2}} \begin{bmatrix} 1 \\ -1 \end{bmatrix} \right) = f\big(\sqrt{r}(R_\theta x)_1\big) e^{-\frac{r(R_\theta x_2)^2}{2}} \begin{bmatrix} e^{-i\theta/2} \\ -e^{i\theta/2} \end{bmatrix}, \qquad f \in \mathcal{S}(\mathbb{R}).$$

This corresponds to (3.14), where we rescaled f by $\sqrt{r}$ (this preserves the Schwartz class). ∎

We define the space

$$\mathcal{S}_{\theta,r}(\mathbb{R}^2) = \left\{ u \in \mathcal{S}(\mathbb{R}^2, \mathbb{C}^2) : \ u \in \ker_{\mathcal{S}(\mathbb{R}^2,\mathbb{C}^2)}(L_{\theta,r})^\perp \right\},$$

with orthogonality computed with respect to the L^2-scalar product. We provide $\mathcal{S}_{\theta,r}(\mathbb{R}^2)$ with the seminorms inherited from $\mathcal{S}(\mathbb{R}^2, \mathbb{C}^2)$.

LEMMA 3.3. *For every $\theta \in \mathbb{R}$ and $r > 0$, the operator $L_{\theta,r}$ acting on $\mathcal{S}_{\theta,r}(\mathbb{R}^2)$ is one to one, with inverse $L_{\theta,r}^{-1}$ bounded on $\mathcal{S}_{\theta,r}(\mathbb{R}^2)$.*

Proof. **1.** We recall that $L_{\theta,r}$ and $\sqrt{r}L_{0,1}$ are conjugated by operators bounded on $\mathcal{S}(\mathbb{R}^2, \mathbb{C}^2)$; see (3.15). Thus, it suffices to prove the lemma for $L_{0,1}$ only.

We introduce the annihilation and creation operators $\mathfrak{a}$ and $\mathfrak{a}^*$, as well as the associated quantum harmonic oscillator $\mathfrak{h} = \mathfrak{a}^*\mathfrak{a}$ and quantum states φ_n:

$$\mathfrak{a} = x_2 + \partial_{x_2}, \quad \mathfrak{a}^* = x_2 - \partial_{x_2}, \quad \mathfrak{h} = -\partial_{x_2}^2 + x_2^2 - 1,$$
$$\varphi_0(x_2) = \frac{1}{\pi^{1/4}} e^{-\frac{x_2^2}{2}}, \quad \varphi_n(x_2) = \frac{(\mathfrak{a}^*)^n}{2^{n/2}\sqrt{n!}}\varphi_0(x_2).$$

The quantum states φ_n form a complete orthonormal basis of eigenvectors of $\mathfrak{h}$: for every n, $\|\varphi_n\|_{L^2} = 1$ and $\mathfrak{h}\varphi_n = 2n\varphi_n$. Moreover they satisfy the creation and annihilation relations: $\mathfrak{a}\varphi_0 = 0$ and for $n \in \mathbb{N}$,

$$\mathfrak{a}^*\varphi_n = \sqrt{2n+2}\varphi_{n+1}, \quad \mathfrak{a}\varphi_{n+1} = \sqrt{2n+2}\varphi_n. \tag{3.17}$$

Introduce

$$\tilde{L}_{0,1} = \begin{bmatrix} 1 & -1 \\ 1 & 1 \end{bmatrix} L_{0,1} \begin{bmatrix} 1 & -1 \\ 1 & 1 \end{bmatrix}^{-1} = \begin{bmatrix} 0 & \mathfrak{a}^* & \mathfrak{a} & 2D_{x_1} \end{bmatrix} \tag{3.18}$$

and the associated space $\tilde{\mathcal{S}}_{0,1}(\mathbb{R}^2)$, defined similarly as $\mathcal{S}_{0,1}(\mathbb{R}^2)$,

$$\tilde{\mathcal{S}}_{0,1}(\mathbb{R}^2) = \left\{ u \in \mathcal{S}(\mathbb{R}^2, \mathbb{C}^2) : \ u \in \ker_{\mathcal{S}(\mathbb{R}^2,\mathbb{C}^2)}(\tilde{L}_{0,1})^\perp \right\}.$$

We observe that $v = (v_1, v_2) \in \ker(\tilde{L}_{0,1})$ if and only if

$$\mathfrak{a}^* v_2 = 0 \text{ and } \mathfrak{a} v_1 + 2D_{x_1} v_2 = 0.$$

This implies $v_2 = 0$ and $v_1(x) = \lambda(x_1)v(x_2)$ for some Schwartz function $x_1 \mapsto \lambda(x_1)$. As a consequence, $u \in \ker_{\mathcal{S}(\mathbb{R}^2,\mathbb{C}^2)}(\tilde{L}_{0,1})^\perp$ if and only if, for all $\lambda \in \mathcal{S}(\mathbb{R})$,

$$\int_{\mathbb{R}^2} \overline{\lambda}(x_1)\varphi_0(x_2)u_1(x_1, x_2)dx_1dx_2 = 0.$$

We obtain

$$\tilde{\mathcal{S}}_{0,1}(\mathbb{R}^2) = \left\{ u \in \mathcal{S}(\mathbb{R}^2, \mathbb{C}^2) : \ \forall x_1 \in \mathbb{R}, \ \int_{\mathbb{R}^2} u_1(x)\varphi_0(x_2)dx_2 = 0 \right\}. \tag{3.19}$$

As a consequence, the lemma boils down to prove that $\tilde{L}_{0,1}$ is invertible on $\tilde{\mathcal{S}}_{0,1}(\mathbb{R}^2)$.

2. Let $\mathcal{W}$ be the Fréchet space of functions $w \in C^\infty(\mathbb{R} \times \mathbb{N}, \mathbb{C}^2)$ such that $w_1(\cdot, 0) = 0$, equipped with the seminorms

$$N_{\alpha,\beta,\gamma}(w) = \sup_{n,\xi} \left| \langle n \rangle^{2\alpha} \langle \xi \rangle^{\beta} \partial_\xi^\gamma w(\xi, n) \right|, \quad \alpha, \beta, \gamma \in \mathbb{N}.$$

We define $S : \tilde{\mathcal{S}}_{0,1}(\mathbb{R}^2) \to \mathcal{W}$ by

$$Su(\xi, n) = \int_{\mathbb{R}^2} e^{-i\xi x_1} \begin{bmatrix} u_1(x)\varphi_{n+1}(x_2) \\ u_2(x)\varphi_n(x_2) \end{bmatrix} dx, \quad u \in \tilde{\mathcal{S}}_{0,1}\big(\mathbb{R}^2\big), \ n \in \mathbb{N}, \ \xi \in \mathbb{R}.$$

We first observe that $S:\tilde{\mathcal{S}}_{0,1}(\mathbb{R}^2)\to\mathcal{W}$ is continuous. Indeed, if $u\in\tilde{\mathcal{S}}_{0,1}(\mathbb{R}^2)$ and $\alpha,\beta,\gamma\in\mathbb{N}$, we have

$$\langle 2n\rangle^{2\alpha}\langle\xi\rangle^{\beta}D_\xi^\gamma Su(\xi,n)=Sv(\xi,n),\qquad v(x)=\langle\mathfrak{h}\rangle^{2\alpha}\langle D_{x_1}\rangle^{\beta}(-x_1)^\gamma u(x).$$

Moreover, $v\in\mathcal{S}(\mathbb{R}^2)$ when $u\in\mathcal{S}(\mathbb{R}^2)$. The Cauchy–Schwarz inequality yields

$$\begin{aligned}N_{\alpha,\beta,\gamma}(Su)=\sup_{n,\xi}\big|Sv(\xi,n)\big|&\le\sup_n\int_{\mathbb{R}^2}\left|\begin{bmatrix}v_1(x)\varphi_{n+1}(x_2)\\ v_2(x)\varphi_n(x_2)\end{bmatrix}\right|dx\\&\le 2\int_{\mathbb{R}}\left(\int_{\mathbb{R}}\big|v(x)\big|^2dx_2\right)^{1/2}dx_1,\end{aligned}$$

where we used $\|\varphi_n\|_{L^2}=1$. The right-hand side (RHS) is controlled by Schwartz seminorms of $v=\langle\mathfrak{h}\rangle^{2\alpha}\langle x_1\rangle^\beta D_{x_1}^\gamma u$, thus of u. Hence S is continuous.

Moreover, S is invertible. The range of S is $\mathcal{W}$: if $w\in\mathcal{W}$, then we have $Su=w$, with

$$u(x)=\frac{1}{2\pi}\int_{\mathbb{R}}e^{i\xi x_1}\sum_{n=0}^{\infty}\left[\varphi_{n+1}(x_2)w_1(\xi,n)\,\varphi_n(x_2)w_2(\xi,n)\right]d\xi,$$

using the Fourier inversion formula and orthogonality relations for the φ_n. We now show that S is one to one. If $u\in\tilde{\mathcal{S}}_{0,1}(\mathbb{R}^2)$ is such that $Su\equiv 0$, then

$$\text{for all } x_1\in\mathbb{R},\ n\in\mathbb{N},\qquad\int_{\mathbb{R}}\begin{bmatrix}u_1(x)\varphi_{n+1}(x_2)\\ u_2(x)\varphi_n(x_2)\end{bmatrix}dx_2=0 \tag{3.20}$$

from the Fourier inversion formula. Since φ_n forms an orthonormal basis of $L^2(\mathbb{R})$, (3.20) implies that $u_2\equiv 0$ and $u_1(x)=c(x_1)\varphi_0(x_2)$. From $u\in\tilde{\mathcal{S}}_{0,1}(\mathbb{R}^2)$ and (3.19), $u_1\equiv 0$. Hence $u\equiv 0$, and S is invertible.

2. We define an operator S by

$$Su(\xi,n)=\int_{\mathbb{R}^2}e^{-i\xi x_1}\begin{bmatrix}u_1(x)\varphi_{n+1}(x_2)\\ u_2(x)\varphi_n(x_2)\end{bmatrix}dx,\qquad u\in\tilde{\mathcal{S}}_{0,1}(\mathbb{R}^2),\ n\in\mathbb{N},\ \xi\in\mathbb{R}.$$

We claim that S is (continuously) invertible from $\tilde{\mathcal{S}}_{0,1}(\mathbb{R}^2)$ to the Fréchet space $\mathcal{V}$ of functions $v\in C^\infty(\mathbb{R}\times\mathbb{N},\mathbb{C}^2)$ such that

$$\text{for all } \alpha,\beta,\gamma\in\mathbb{N},\quad N_{\alpha,\beta,\gamma}(v)=\sup_{n,\xi}\left|\langle n\rangle^{2\alpha}\langle\xi\rangle^{\beta}\partial_\xi^\gamma v(\xi,n)\right|<\infty.$$

This boils down to proving that if $u\in\tilde{\mathcal{S}}_{0,1}(\mathbb{R}^2)$, then, for every $\alpha,\beta,\gamma\in\mathbb{N}$, the quantity $N_{\alpha,\beta,\gamma}(Su)$ is controlled by finitely many seminorms of u in $\mathcal{S}(\mathbb{R}^2,\mathbb{C}^2)$, and conversely.

We first observe that, for $u\in\mathcal{S}_{0,1}(\mathbb{R}^2)$ and $\alpha,\beta,\gamma\in\mathbb{N}$,

$$\langle n\rangle^{2\alpha}\langle\xi\rangle^{\beta}\partial_\xi^\gamma Su(\xi,n)=Sv(\xi,n),\qquad v(x)=\langle\mathfrak{h}\rangle^{2\alpha}\langle D_{x_1}\rangle^{\beta}x_1{}^\gamma u(x).$$

Moreover, $v\in\mathcal{S}(\mathbb{R}^2,\mathbb{C}^2)$ whenever $u\in\mathcal{S}(\mathbb{R}^2,\mathbb{C}^2)$. Therefore,

$$\begin{aligned}N_{\alpha,\beta,\gamma}(Su)=\sup_{n,\xi}\big|Sv(\xi,n)\big|&\le\sup_n\int_{\mathbb{R}^2}\left|\begin{bmatrix}v_1(x)\varphi_{n+1}(x_2)\\ v_2(x)\varphi_n(x_2)\end{bmatrix}\right|dx\\&\le 2\int_{\mathbb{R}}\left(\int_{\mathbb{R}}\big|v(x)\big|^2dx_2\right)^{1/2}dx_1,\end{aligned}$$

where we applied the Cauchy–Schwarz inequality and the fact that $\|\varphi_n\|_{L^2} = 1$. The RHS is controlled by seminorms in $\mathcal{S}(\mathbb{R}^2, \mathbb{C}^2)$ of $v = \langle \mathfrak{h} \rangle^{2\alpha} \langle x_1 \rangle^{\beta} D_{x_1}^{\gamma} u$ and thus of u.

We now prove the backward implication. Assume that $u \in \tilde{\mathcal{S}}_{0,1}(\mathbb{R}^2)$ satisfies

$$\text{for all } \alpha, \beta, \gamma \in \mathbb{N}, \quad N_{\alpha,\beta,\gamma}(Su) < \infty.$$

We use the Fourier inversion formula and the fact that the φ_n form an orthonormal basis to deduce that

$$u(x) = \frac{1}{2\pi} \int_{\mathbb{R}} e^{i\xi x_1} \sum_{n=0}^{\infty} \left[\varphi_{n+1}(x_2)(Su)_1(\xi, n)\, \varphi_n(x_2)(Su)_2(\xi, n) \right] d\xi.$$

Let us prove that, for all $\alpha, \beta \in \mathbb{N}^2$, the function $x^{\alpha} \partial_x^{\beta} u$ is in L^2 (which will yields that u is Schwartz class). For this, we consider the term of the series that constitutes its coordinates. For $j \in \{1, 2\}$ and $n \in \mathbb{N}$, we have

$$\begin{aligned} &x^{\alpha} \partial_x^{\beta} \left(\int_{\mathbb{R}} e^{i\xi x_1} \varphi_{n+1}(x_2)(Su)_j(\xi, n) d\xi \right) \\ &\quad = \int_{\mathbb{R}} x_1^{\alpha_1} (i\xi)^{\beta} e^{i\xi x_1} x_2^{\alpha_2} \partial_{x_2}^{\beta_2} \varphi_{n+1}(x_2)(Su)_j(\xi, n) d\xi. \end{aligned}$$

An integration by parts gives

$$\begin{aligned} &x^{\alpha} \partial_x^{\beta} \left(\int_{\mathbb{R}} e^{i\xi x_1} \varphi_{n+1}(x_2)(Su)_j(\xi, n) d\xi \right) \\ &\quad = i^{\alpha_1 + \beta_1} \int_{\mathbb{R}} e^{i\xi x_1} x_2^{\alpha_2} \partial_{x_2}^{\beta_2} \varphi_{n+1}(x_2) \partial_{\xi}^{\alpha_1} (\xi^{\beta_1} (Su)_j(\xi, n)) d\xi. \end{aligned}$$

Besides, using $x_2 = \mathfrak{a} + \mathfrak{a}^*$ and $\partial_{x_2} = \mathfrak{a} - \mathfrak{a}^*$, we deduce from (3.17) the existence of a constant $C_{\alpha_2,\beta_2} > 0$ such that

$$\|x_2^{\alpha_2} \partial_{x_2}^{\beta_2} \varphi_{n+1}(x_2)\|_{L^2} \leq C_{\alpha_2,\beta_2} n^{\frac{\alpha_2 + \beta_2}{2}}.$$

As a consequence, for $j \in \{1, 2\}$ and $n \in \mathbb{N}$, we have

$$\begin{aligned} \left\| x^{\alpha} \partial_x^{\beta} \left(\int_{\mathbb{R}} e^{i\xi x_1} \varphi_{n+1}(x_2)(Su)_j(\xi, n) d\xi \right) \right\|_{L^2} &\leq n^{-2} C_{\alpha_2,\beta_2} \left(\int_{\mathbb{R}} \langle \xi \rangle^{-2} d\xi \right) \\ &\quad \sup_{n,\xi} \left| n^{\frac{\alpha_2 + \beta_2}{2} + 2} \langle \xi \rangle^{\beta_1 + 2} \partial_{\xi}^{\alpha_1} (Su)_j(\xi, n) \right|, \end{aligned}$$

whence the convergence of the series in L^2 and a control of the L^2 norm of $x^{\alpha} \partial_x^{\beta} u$ by the seminorms of $Su(\xi, n)$. From $x^{\alpha} \partial_x^{\beta} f \in L^2$ for all α, β, we conclude that $f \in \mathcal{S}(\mathbb{R}^2)$.

Besides, because of the closed graph theorem, invertible continuous operators between Fréchet spaces have continuous inverses. Hence the inverse of S is continuous from $\mathcal{W}$ to $\tilde{\mathcal{S}}_{0,1}(\mathbb{R}^2)$.

3. Let us now conclude the proof. As we have seen in step 1, to prove the lemma it suffices to show that $\tilde{L}_{0,1}$ is invertible on $\tilde{\mathcal{S}}_{0,1}(\mathbb{R}^2)$. By step 2, S is continuous invertible from $\tilde{\mathcal{S}}_{0,1}(\mathbb{R}^2)$ to $\mathcal{W}$. Thus, we only have to prove that $S\tilde{L}_{0,1}S^{-1} : \mathcal{W} \to \mathcal{W}$ is invertible with bounded inverse. But $S\tilde{L}_{0,1}S^{-1}$ is actually a simple multiplication operator: using that D_{x_1} corresponds to ξ in Fourier space and $\mathfrak{a}, \mathfrak{a}^*$ are shift operators—see (3.17)—in Hermite space, we have

$$S\tilde{L}_{0,1}S^{-1} w(\xi, n) = \begin{bmatrix} 0 & \sqrt{2n+2} \\ \sqrt{2n+2} & 2\xi \end{bmatrix} w(\xi, n). \tag{3.21}$$

This is a continuous operator on $\mathcal{W}$, and (3.21) yields a formula for $\tilde{L}_{0,1}^{-1}$:

$$\tilde{L}_{0,1}^{-1} = S^{-1}\frac{1}{2n+2}\begin{bmatrix} 2\xi & -\sqrt{2n+2} \\ -\sqrt{2n+2} & 0 \end{bmatrix} S.$$

This completes the proof. ∎

3.4. Solving the dominant equation. We now focus on solving the hierarchy of equations (3.9), starting with the first two:

$$T_0 a_0 = 0, \quad T_0 a_1 + T_1 a_0 = 0.$$

Below we abuse notation: we allow functions in $\mathcal{S}(\mathbb{R})$ or $\mathcal{S}(\mathbb{R}^2, \mathbb{C}^2)$ to also depend smoothly on time, and we consider the operator $\mathcal{K}_t$ from (3.3) on functions depending on t. For instance, we write (3.22) as

$$a_0(t,x) = \mathcal{K}_t f_0(t,x) = r_t^{1/4} f_0\big(t, (R_{\theta_t}x)_1\big) e^{-\frac{r_t (R_{\theta_t}x)_2^2}{2}} \begin{bmatrix} e^{-i\theta_t/2} \\ -e^{i\theta_t/2} \end{bmatrix}. \tag{3.22}$$

Since $T_0 = L_{\theta_t, r_t}$, Lemma 3.2 implies that, for any $f_0 \in \mathcal{S}(\mathbb{R})$ (potentially depending on t), (3.22) solves the equation $T_0 a_0 = 0$.

3.5. Solving the subleading equation. The subleading equation in the hierarchy (3.9) is $T_0 a_1 + T_1 a_0 = 0$, where $T_0 = L_{\theta_t, r_t}$ and

$$T_1 = D_t + \sum_{|\alpha|=2} \frac{\partial^\alpha \kappa(y_t)}{\alpha!} x^\alpha \sigma_3. \tag{3.23}$$

Given a_0 satisfying (3.22), we regard $T_0 a_1 + T_1 a_0 = 0$ as an equation with unknown $a_1 \in \mathcal{S}(\mathbb{R}^2, \mathbb{C}^2)$. According to Lemma 3.3, a solution exists if, for any $t \in \mathbb{R}$, $T_1 a_0(t, \cdot) \in \mathcal{S}_{\theta_t, r_t}(\mathbb{R}^2)$. We now look for f_0 such that this holds.

We note that $T_1 a_0 \in \mathcal{S}_{\theta_t, r_t}(\mathbb{R}^2)$ if and only if, for every $t \in \mathbb{R}$ and $g \in \mathcal{S}(\mathbb{R})$,

$$\int_{\mathbb{R}^2} g\big((R_{\theta_t}x)_1\big) e^{-\frac{r_t (R_{\theta_t}x)_2^2}{2}} \begin{bmatrix} e^{i\theta_t/2} \\ -e^{-i\theta_t/2} \end{bmatrix} \cdot T_1 a_0(t,x) dx = 0. \tag{3.24}$$

We make the substitution $x \mapsto R_{\theta_t}^\top x$ and pick functions g approaching delta distributions to obtain that (3.24) is equivalent to

$$\text{for all } t, x_1 \in \mathbb{R}, \quad \int_{\mathbb{R}} e^{-\frac{r_t x_2^2}{2}} \begin{bmatrix} e^{i\theta_t/2} \\ -e^{-i\theta_t/2} \end{bmatrix} \cdot (T_1 a_0)\big(t, R_{\theta_t}^\top x\big) dx_2 = 0. \tag{3.25}$$

LEMMA 3.4. *If $f(t,\cdot) \in \mathcal{S}(\mathbb{R})$ depends smoothly on t, then*

$$\int_{\mathbb{R}} e^{-\frac{r_t x_2^2}{2}} \begin{bmatrix} e^{i\theta_t/2} \\ -e^{-i\theta_t/2} \end{bmatrix} \cdot (T_1 \mathcal{K}_t f)\big(t, R_\theta^\top x\big) dx_2 = 2\sqrt{\frac{\pi}{r_t}} D_t f(t, x_1). \tag{3.26}$$

Proof. We note the identities

$$\left\langle \begin{bmatrix} e^{-i\theta_t/2} \\ -e^{i\theta_t/2} \end{bmatrix}, \sigma_3 \begin{bmatrix} e^{-i\theta_t/2} \\ -e^{i\theta_t/2} \end{bmatrix} \right\rangle = 0, \quad \left\langle \begin{bmatrix} e^{-i\theta_t/2} \\ -e^{i\theta_t/2} \end{bmatrix}, \begin{bmatrix} -\dot{\theta}_t e^{-i\theta_t/2} \\ -\dot{\theta}_t e^{i\theta_t/2} \end{bmatrix} \right\rangle = 0. \tag{3.27}$$

Therefore, using the expressions (3.23) for T_1 and (3.3) for $\mathcal{K}_t$, we have

$$\begin{aligned}(3.28)\qquad \begin{bmatrix} e^{i\theta_t/2} \\ -e^{-i\theta_t/2}\end{bmatrix} \cdot T_1\mathcal{K}_t f(t,x) &= 2D_t\left(r_t^{1/4} f\big(t,(R_{\theta_t}x)_1\big)e^{-\frac{r_t(R_{\theta_t}x)_2^2}{2}}\right)\\ &= \frac{2}{i}e^{-\frac{r_t(R_{\theta_t}x)_2^2}{2}}\left(\frac{\partial}{\partial t} + (\dot{R_{\theta_t}}x)_1\frac{\partial}{\partial x_1} - \frac{\dot{r_t}(R_{\theta_t}x)_2^2}{2}\right.\\ &\quad \left. - r_t(R_{\theta_t}x)_2(\dot{R_{\theta_t}}x)_2\right) r_t^{1/4} f\big(t,(R_{\theta_t}x)_1\big).\end{aligned}$$

We deduce that

$$\begin{aligned}(3.29)\qquad &\begin{bmatrix} e^{i\theta_t/2} \\ -e^{-i\theta_t/2}\end{bmatrix} \cdot T_1\mathcal{K}_t f(t,R_{\theta_t}^\top x)\\ &\quad = -2ie^{-\frac{r_t x_2^2}{2}}\left(\frac{\partial}{\partial t} + (\dot{R_{\theta_t}}R_{\theta_t}^\top x)_1\frac{\partial}{\partial x_1} - \frac{\dot{r_t}x_2^2}{2} - r_t x_2(\dot{R_{\theta_t}}R_{\theta_t}^\top x)_2\right) r_t^{1/4} f\big(t,x_1\big).\end{aligned}$$

We remark that

$$(3.30)\qquad \dot{R_{\theta_t}}\cdot R_\theta^\top x = \dot{\theta}_t\begin{bmatrix} 0 & 1 \\ -1 & 0\end{bmatrix} x = \dot{\theta}_t\begin{bmatrix} x_2 \\ -x_1\end{bmatrix}.$$

We deduce that (3.29) becomes

$$\begin{bmatrix} e^{i\theta_t/2} \\ -e^{-i\theta_t/2}\end{bmatrix} T_1\mathcal{K}_t f(t,R_{\theta_t}^\top x) = -2ie^{-\frac{r_t x_2^2}{2}}\left(\frac{\partial}{\partial t} + \dot{\theta}_t x_2\frac{\partial}{\partial x_1} - \frac{\dot{r_t}x_2^2}{2} + r_t\dot{\theta}_t x_2 x_1\right) r_t^{1/4} f\big(t,x_1\big).$$

We plug this identity in (3.26) to obtain

$$(3.31)\qquad -2i\int_{\mathbb{R}} e^{-r_t x_2^2}\left(\frac{\partial}{\partial t} + \dot{\theta}_t x_2\frac{\partial}{\partial x_1} - \frac{\dot{r_t}x_2^2}{2} + r_t\dot{\theta}_t x_2 x_1\right) dx_2 \cdot r_t^{1/4} f\big(t,x_1\big).$$

We now perform the integrals over x_2. The function $x_2 e^{-r_t x_2^2}$ has vanishing integral; moreover an integration by parts shows that

$$\sqrt{\frac{\pi}{r_t}} = \int_{\mathbb{R}} e^{-r_t x_2^2} dx_2 = 2r_t\cdot\int_{\mathbb{R}} x_2^2 e^{-r_t x_2^2} dx_2.$$

Hence (3.31) reduces to

$$(3.32)\qquad -2i\sqrt{\frac{\pi}{r_t}}\left(\frac{\partial}{\partial t} - \frac{\dot{r_t}}{4r_t}\right) r_t^{1/4} f\big(t,x_1\big).$$

We finally observe that in the sense of differential operators,

$$\left(\frac{\partial}{\partial t} - \frac{\dot{r_t}}{4r_t}\right) r_t^{1/4} = \frac{\partial}{\partial t}.$$

Using this identity in (3.32) completes the proof. ∎

From (3.25) and Lemma 3.4, we obtain the transport equation for f_0: $D_t f_0 = 0$. Hence, f_0 depends on x_1 only, and we write $f_0(t,x_1) = f_0(x_1)$. Therefore, if

$$(3.33)\qquad a_0(t,x) = r_t^{1/4} f_0\big((R_{\theta_t}x)_1\big)e^{-\frac{r_t(R_{\theta_t}x)_2^2}{2}}\begin{bmatrix} e^{-i\theta_t/2} \\ -e^{i\theta_t/2}\end{bmatrix} = \mathcal{K}_t f_0(x)$$

for some $f_0 \in \mathcal{S}(\mathbb{R})$, then $T_1 a_0(t,\cdot) \in \mathcal{S}_{\theta_t,r_t}(\mathbb{R}^2)$ for every $t \in \mathbb{R}$; hence the equation $T_0 b_1 + T_1 a_0 = 0$ has a unique solution b_1 such that $b_1(t,\cdot) \in \mathcal{S}_{\theta_t,r_t}(\mathbb{R}^2)$ for every $t \in \mathbb{R}$. We obtain the general solution to $T_0 a_1 + T_1 a_0 = 0$ by adding an element of $\ker(L_{\theta_t,r_t})$: $a_1 = b_1 + \mathcal{K}_t f_1$:

$$a_1(t,x) = b_1(t,x) + r_t^{1/4} f_1\big(t,(R_{\theta_t}x)_1\big) e^{-\frac{r_t (R_{\theta_t}x)_2^2}{2}} \begin{bmatrix} e^{-i\theta_t/2} \\ -e^{i\theta_t/2} \end{bmatrix}, \qquad f_1(t,\cdot) \in \mathcal{S}(\mathbb{R}). \tag{3.34}$$

3.6. Proof of Theorem 2. We are now in a position to prove Theorem 2. We start with a classical result based on Duhamel's formula.

LEMMA 3.5. *Let $\psi_t \in \mathcal{S}(\mathbb{R}^2)$ be a solution to $(\varepsilon D_t + H)\psi_t = 0$. Then, for any $v_t \in \mathcal{S}(\mathbb{R}^2)$,*

$$\big\|v_t - \psi_t\big\|_{L^2} \le \|v_0 - \psi_0\|_{L^2} + \frac{1}{\varepsilon}\int_0^t \big\|(\varepsilon D_s + H)v_s\big\|_{L^2} ds.$$

Proof. Let $w_t = v_t - \psi_t$ and $r_t = (\varepsilon D_t + H)v_t$. Then, $(\varepsilon D_t + H)w_t = r_t$. By Duhamel's formula,

$$v_t - \psi_t = w_t = e^{-itH/\varepsilon} w_0 + \frac{1}{\varepsilon}\int_0^t e^{-i(t-s)H/\varepsilon} r_s ds = e^{-itH/\varepsilon}(v_0 - \psi_0) + \frac{1}{\varepsilon}\int_0^t e^{-i(t-s)H/\varepsilon} r_s ds.$$

We bound both sides in L^2, using that e^{-itH} is unitary:

$$\|v_t - \psi_t\|_{L^2} \le \|v_0 - \psi_0\|_{L^2} + \frac{1}{\varepsilon}\int_0^t \big\|(\varepsilon D_s + H)v_s\big\|_{L^2} ds.$$

This completes the proof. ∎

Proof of Theorem 2. **1.** Let $f_0 \in \mathcal{S}(\mathbb{R})$. Let a_0 as in (3.22), b_1 is as in (3.34), and $a^{(1)} = a_0 + \varepsilon^{1/2} a_1$. We apply Lemma 3.1 with $m = 1$:

$$\big\|(\varepsilon D_t + H) W[a^{(1)}]_{y_t}\big\|_{L^2} \le C\varepsilon^{3/2}\left(\|D_t b_1\|_{L^2} + \big\|\langle x\rangle^3 a_0\big\|_{L^2} + \big\|\langle x\rangle^3 b_1\big\|_{L^2}\right). \tag{3.35}$$

2. We now bound the RHS of (3.35), starting with $\langle x\rangle^3 a_0$ in L^2. We write $a_0 = \mathcal{K}_{\theta_t,r_t} f_0$, where

$$\mathcal{K}_{\theta,r} f(x) = r^{1/4} f\big((R_\theta x)_1\big) e^{-\frac{r(R_\theta x)_2^2}{2}} \begin{bmatrix} e^{-i\theta/2} \\ -e^{i\theta/2} \end{bmatrix}, \ f \in \mathcal{S}(\mathbb{R}).$$

We note that we have the identity $\mathcal{K}_{\theta,r} = \mathcal{D}_r \mathcal{U}_\theta \mathcal{K}_{0,1}$, where $\mathcal{U}_\theta$ was introduced in (2.2) and $\mathcal{D}_r$ is a partial dilation operator:

$$\mathcal{D}_r \psi(x) = r^{1/4}\psi\left(x_1, \sqrt{r}x_2\right), \qquad \mathcal{U}_\theta \psi(x) = \begin{bmatrix} e^{-i\theta/2} & 0 \\ 0 & e^{i\theta/2} \end{bmatrix} \psi(R_\theta x), \ \psi \in \mathcal{S}(\mathbb{R}^2). \tag{3.36}$$

The operator $\mathcal{K}_{0,1}$ is bounded from $\mathcal{S}(\mathbb{R})$ to $\mathcal{S}(\mathbb{R}^2, \mathbb{C}^2)$; $\mathcal{U}_\theta$ is uniformly bounded from $\mathcal{S}(\mathbb{R}^2)$ to $\mathcal{S}(\mathbb{R}^2, \mathbb{C}^2)$ for $\theta \in \mathbb{R}$; and $\mathcal{D}_r$ is bounded uniformly on $\mathcal{S}(\mathbb{R}^2)$ for r in compact subsets of $(0,\infty)$. Moreover, $r_t = |\nabla\kappa(y_t)|$ lives in a compact subset of $(0,\infty)$ because of $\nabla\kappa \in C_b^\infty(\mathbb{R}^2)$ and (3.1). We deduce that $a_0 \in \mathcal{S}(\mathbb{R}^2)$, with uniform-in-time bounds on its seminorms. In particular, $\|\langle x\rangle^3 a_0\|_{L^2}$ is uniformly bounded.

For later use, we observe that $\partial_t a_0$ is also uniformly bounded in $\mathcal{S}(\mathbb{R}^2)$. Indeed, from (3.36), we have

$$\partial_t a_0 = \dot{r}_t \partial_r \mathcal{D}_{r_t} \mathcal{U}_{\theta_t} \mathcal{K}_{0,1} f_0 + \dot{\theta}_t \mathcal{D}_{r_t} \partial_\theta \mathcal{U}_{\theta_t} \mathcal{K}_{0,1} f_0. \tag{3.37}$$

The operators $\partial_\theta \mathcal{U}_{\theta_t}$ and $\partial_r \mathcal{D}_{r_t}$ are uniformly bounded on $\mathcal{S}(\mathbb{R}^2)$—the latter because r_t lives in a compact subset of $(0,\infty)$. The quantities $\dot{r}_t$ and $\dot{\theta}_t$ are uniformly bounded; indeed, by (3.2),

$$|\dot{r}_t| = \frac{|\langle \nabla\kappa(y_t), \nabla^2\kappa(y_t)\dot{y}_t\rangle|}{|\nabla\kappa(y_t)v(y_t)|} \le |\nabla^2\kappa(y_t)\dot{y}_t| \le C,$$

and likewise,

$$|\dot{\theta}_t| = \left|\frac{d}{dt}\frac{\nabla\kappa(y_t)}{r_t}\right| \le \frac{|\dot{r}_t|}{r_t} + \frac{|\nabla^2\kappa(y_t)v(y_t)|}{r_t} \le C,$$

where we have used $|v(y_t)| = 1$ and the fact that r_t is bounded below and the derivatives of κ are bounded (here $\nabla^2\kappa$ denotes the matrix of second order partial derivatives of κ).

Therefore, we deduce from (3.37) that $\partial_t a_0$ is uniformly bounded in $\mathcal{S}(\mathbb{R}^2)$.

3. We now control in L^2 the terms $D_t b_1$ and $\langle x\rangle^3 b_1$ that appear in (3.35). We use (3.15) to write b_1 as

$$b_1(t,\cdot) = -L^{-1}_{\theta_t,r_t} a_0 = -\sqrt{r_t} S^{-1}_{r_t} \mathcal{U}^{-1}_{\theta_t} L^{-1}_{0,1} \mathcal{U}_{\theta_t} S_{r_t} a_0. \tag{3.38}$$

As in step 2, all operators involved in (3.38) are uniformly bounded in $\mathcal{S}(\mathbb{R}^2)$, and we deduce that $b_1 \in \mathcal{S}(\mathbb{R}^2)$ uniformly in time. Also similarly to (3.37), taking time derivatives produces quantities such as $\dot{r}_t$, $r_t^{-1/2}$, $\dot{\theta}_t$ (all uniformly bounded); operators such as $\partial_r \mathcal{D}_{r_t}, \partial_r \mathcal{D}_{r_t^{-1}}$, $\partial_\theta \mathcal{U}_{\theta_t}$, and $\partial_\theta \mathcal{U}_{-\theta_t}$, all uniformly bounded on $\mathcal{S}(\mathbb{R}^2)$; and the function $\partial_t a_0$—also bounded uniformly in $\mathcal{S}(\mathbb{R}^2)$. We deduce that $b_1, \partial_t b_1$ are uniformly in $\mathcal{S}(\mathbb{R}^2)$. Hence, $\|\langle x\rangle^3 b_1\|_{L^2}$ and $\|\partial_t b_1\|_{L^2}$ are uniformly bounded.

4. Going back to (3.35), we have, for any t

$$\left\|(\varepsilon D_t + H) W[a^{(1)}]_{y_t}\right\|_{L^2} \le C\varepsilon^{3/2}. \tag{3.39}$$

Let ψ_t be the solution to $(\varepsilon D_t + H)\psi_t = 0$ with initial data $\psi_0 = a_0(0,\cdot)$, and $v_t = W[a^{(1)}]_{y_t}$. We note that $v_0 - \psi_0 = \varepsilon^{1/2} b_1(0,\cdot)$ and that v_t satisfies the bound (3.39). Thanks to Lemma 3.5, we get

$$\|v_t - \psi_t\|_{L^2} \le \varepsilon^{1/2}\|b_1(0,\cdot)\|_{L^2} + C\varepsilon^{1/2} t.$$

Therefore,

$$\psi_t = W[a^{(1)}]_{y_t} + \mathcal{O}_{L^2}\left(\varepsilon^{1/2}\langle t\rangle\right) = W[a_0]_{y_t} + \mathcal{O}_{L^2}\left(\varepsilon^{1/2}\langle t\rangle\right).$$

This completes the proof. ∎

3.7. Subsequent equations. We now focus on deriving a version of Theorem 2 that favors accuracy over lifetime. This requires to solve higher-order transport equations.

The base case is the result of section 3.4–3.5, summarized as follows:

($\mathbf{H_1}$) For any $f_0 \in \mathcal{S}(\mathbb{R})$, there exists b_1 such that, for any $f_1(t,\cdot) \in \mathcal{S}(\mathbb{R})$, if $a_0 = \mathcal{K}_t f_0$ and $a_1 = b_1 + \mathcal{K}_t f_1$, then a_0 and a_1 solve (3.9) with $m = 1$, i.e.,

$$\sum_{\ell=0}^{j} T_{j-\ell} a_j = 0, \quad 0 \le j \le 1.$$

To construct a_0 and a_1, we had to enforce a condition on f_0. Likewise, to construct a_m we will enforce a condition on f_{m-1}.

Our inductive assumption is, for $m \geq 1$, as follows:

$(\mathbf{H_m})$ For any $f_0 \in \mathcal{S}(\mathbb{R})$, there exist $b_1, f_1, \ldots, b_{m-1}, f_{m-1}, b_m \in \mathcal{S}(\mathbb{R})$ depending smoothly on t such that, for any $f_m \in \mathcal{S}(\mathbb{R})$, if $a_0 = \mathcal{K}_t f_0$ and $a_\ell = b_\ell + \mathcal{K}_t f_\ell$, then

$$\sum_{\ell=0}^{j} T_{j-\ell} a_j = 0, \quad 0 \leq j \leq m.$$

We proved $\mathbf{(H_1)}$ in section 3.5. We now assume that $\mathbf{(H_{m-1})}$ holds, and we prove $\mathbf{(H_m)}$ for $m \geq 2$. Because of Lemma 3.1, this boils down to constructing $a_m = b_m + \mathcal{K}_t f_m$ such that

$$T_0(b_m + \mathcal{K}_t f_m) + T_1 a_{m-1} + \cdots + T_m a_0 = 0, \quad \text{where} \tag{3.40}$$

- the operators T_k are defined in (3.8);
- he amplitudes $a_0, \ldots, a_{m-2}$ are fully specified by $\mathbf{(H_{m-1})}$;
- the amplitude $a_{m-1} = b_{m-1} + \mathcal{K}_t f_{m-1}$, with b_{m-1} given by $\mathbf{(H_{m-1})}$ and $f_{m-1} \in \mathcal{S}(\mathbb{R})$, remains to be selected.

Since the operator $\mathcal{K}_t$ parametrizes the kernel of T_0, (3.40) is equivalent to

$$T_0 b_m = \beta_{m-1} - T_1 \mathcal{K}_t f_{m-1}, \quad \beta_{m-1} = -T_1 b_{m-1} - T_2 a_{m-2} - \cdots - T_m a_0. \tag{3.41}$$

Note that $\mathbf{(H_{m-1})}$ fully prescribes β_{m-1}.

As in section 3.5, to solve (3.41), it suffices that, for any t, $(\beta_{m-1} - T_1 \mathcal{K}_t f_{m-1})(t, \cdot)$ is in the kernel of T_0. This is equivalent to,

$$\text{for all } t, x_1 \in \mathbb{R}, \quad \int_{\mathbb{R}} e^{-\frac{r_t x_2^2}{2}} \begin{bmatrix} e^{i\theta_t/2} \\ -e^{-i\theta_t/2} \end{bmatrix} \cdot \big(\beta_{m-1} - T_1 \mathcal{K}_t f_{m-1}\big)\big(t, R_{\theta_t}^\top x\big) dx_2 = 0.$$

Thanks to Lemma 3.4, this is equivalent to

$$D_t f_{m-1}(t, x_1) = \frac{1}{2}\sqrt{\frac{r_t}{\pi}} \int_{\mathbb{R}} e^{-\frac{r_t x_2^2}{2}} \begin{bmatrix} e^{i\theta_t/2} \\ -e^{-i\theta_t/2} \end{bmatrix} \cdot \beta_{m-1}\big(t, R_{\theta_t}^\top x\big) dx_2, \tag{3.42}$$

and hence, setting $f_{m-1}(0, x_1) = 0$,

$$f_{m-1}(t, x_1) = \int_0^t \int_{\mathbb{R}} \frac{1}{2}\sqrt{\frac{r_s}{\pi}} e^{-\frac{r_s x_2^2}{2}} \begin{bmatrix} e^{i\theta_s/2} \\ -e^{-i\theta_s/2} \end{bmatrix} \cdot \beta_{m-1}\big(s, R_{\theta_s}^\top x\big) dx_2 ds. \tag{3.43}$$

When f_{m-1} is given by this formula, (3.41) admits a solution $b_m(t, \cdot) \in \mathcal{S}(\mathbb{R}^2, \mathbb{C}^2)$. This completes the proof of $\mathbf{(H_m)}$. The following result summarizes our findings.

THEOREM 3. *Fix $T > 0$ and $n \in \mathbb{N}$. If $a_j \in \mathcal{S}(\mathbb{R}^2)$ are constructed as above, then $(\varepsilon D_t + H)\phi_t = 0$ has a solution of the form*

$$\phi_t(x) = \frac{1}{\sqrt{\varepsilon}} \cdot \mathcal{K}_t f\left(\frac{x - y_t}{\sqrt{\varepsilon}}\right) + \sum_{j=1}^{n} \varepsilon^{\frac{j-1}{2}} a_j\left(t, \frac{x - y_t}{\sqrt{\varepsilon}}\right) + \mathcal{O}_{L^2}\big(\varepsilon^{\frac{n+1}{2}}\big), \tag{3.44}$$

uniformly for $\varepsilon \in (0, 1]$ and t in $[0, T]$.

According to Theorem 3, after adequately correcting the initial data (3.4) we obtain approximate solutions concentrated near y_t at arbitrary accuracy in ε. In

particular, this indicates that the mass that dissipates in the bulk (i.e., away from κ) is at most $O(\varepsilon^N)$ for any N. For this result, it is necessary to prepare the initial data suitably, otherwise the subleading amplitude (which is of order $\varepsilon^{1/2}$) likely contains a dispersive part; according to Conjecture 2 part of its mass should disperse along Γ.

Remark 2 (timescale of validity of error estimates). Including higher-order correctors as in (3.44) does not extend the timescale of validity $\varepsilon^{-1/2}$ of the approximation solution. Indeed, the nth corrector is of order $\varepsilon^{\frac{n+1}{2}}t^n$—the term t^n corresponds to n recursive integrations in (3.43). After applying Lemma 3.5, this yields that the constant implicitly involved in the remainder $\mathcal{O}_{L^2}\big(\varepsilon^{\frac{n+1}{2}}\big)$ of (3.44) grows like T^{n+1}: it is small only for $T \ll \varepsilon^{-1/2}$.

Proof of Theorem 3. Fix $n \in \mathbb{N}$, $T > 0$, and $f_0 \in \mathcal{S}(\mathbb{R})$. We pick a_j solving (3.9) for $0 \le j \le n+1$ (constructed above) with $f_{n+1} = 0$, and we define

$$a^{(n)} = \sum_{j=0}^{n+1} \varepsilon^{j/2} a_j, \qquad v_t(x) = W\big[a^{(n)}\big]_{y_t}(x) = \frac{1}{\sqrt{\varepsilon}} \sum_{j=0}^{n+1} \varepsilon^{j/2} a_j \left(t, \frac{x - y_t}{\sqrt{\varepsilon}}\right). \tag{3.45}$$

By construction, the functions a_j are smooth in t and Schwartz in x. In particular, they satisfy uniform Schwartz-class bounds for t in compact intervals. Hence, thanks to Lemma 3.1, we have uniformly in $t \in [0, T]$

$$\|(\varepsilon D_t + H) v_t\|_{L^2} \le C\varepsilon^{\frac{n+1}{2}}.$$

Let ϕ_t be the solution to $(\varepsilon D_t + H)\phi_t = 0$ with $\phi_0 = v_0$; see (3.45) with $t = 0$. Thanks to Lemma 3.5,

$$\|v_t - \phi_t\|_{L^2} \le C\varepsilon^{\frac{n+1}{2}}.$$

In other words, $v_t = \phi_t + \mathcal{O}_{L^2}\big(\varepsilon^{\frac{n+1}{2}}\big)$. ∎

4. The effect of curvature. It is natural to wonder which quantities affect the lifetime of our quantum state. For instance, when κ is linear, the interface is straight and the edge states have infinite lifetime. If κ is asymptotically linear, the interface is asymptotically straight and we expect an extended time of validity. In contrast, numerical simulations indicate that circular interfaces come with gradual dispersion; see Figure 2.

This suggests that an integrated curvature limits the lifespan. Curvature, however, cannot be the only limiting factor: as Figure 5 shows, even straight interfaces can generate dispersion. To isolate the effects of curvature, we consider in this section domain walls κ that satisfy a geometric condition

$$y \in \kappa^{-1}(0) \quad \Rightarrow \quad \big|\nabla\kappa(y)\big| = 1, \qquad \nabla^2\kappa(y) \cdot \nabla\kappa(y) = 0. \tag{4.1}$$

Examples of κ satisfying (4.1) include

- $\kappa(x) = \omega \cdot x$ with $|\omega| = 1$ for a straight interface;
- $\kappa(x) = \sqrt{x_1^2 + x_2^2} - 1$ for a circle.

The condition (4.1) is not geometrically restrictive: given Γ, we can always find κ with $\Gamma = \kappa^{-1}(0)$, satisfying (4.1); see section 4.2. This condition excludes scenarios such as those giving rise to Figure 5. Under (4.1), $\dot\theta_t$ is the curvature of Γ at y_t, and in a suitable frame, the Hessian of κ along Γ depends only on $\dot\theta_t$:

$$\big\langle R_{\theta_t}^\top x, \nabla^2\kappa(y_t) R_{\theta_t}^\top x \big\rangle = \dot\theta_t x_1^2. \tag{4.2}$$

THEOREM 4. *Under* (4.1), *the solution* (1.4) *to* $(\varepsilon D_t + H)\Psi_t = 0$ *of Theorem* 1 *satisfies, uniformly in* $t > 0$ *and* $\varepsilon \in (0, 1]$,

(4.3)
$$\Psi_t(x) = \frac{1}{\sqrt{\varepsilon}} \cdot \exp\left(-\frac{(x - y_t)^2}{2\varepsilon}\right) \begin{bmatrix} -e^{i\theta_t/2} \\ e^{-i\theta_t/2} \end{bmatrix} + \mathcal{O}_{L^2}\left(\varepsilon^{1/2} + \varepsilon t(1 + \Theta_t)\right), \qquad \Theta_t = \int_0^t \dot{\theta}_s^2 ds.$$

When Γ is asymptotically straight (i.e., it has L^2-curvature), the remainder in (4.3) remains small for $t \ll \varepsilon^{-1}$: our quantum state is longer-lived. In contrast, if Γ is a closed loop, then Θ_t grows linearly and our state is only close to the exact solution for $\varepsilon t^2 \ll 1$; that is, $t \ll \varepsilon^{-1/2}$: there is no improvement over Theorem 1. Thus, such states—which are not globally topological—have a shorter lifetime.

Theorem 4 highlights effective limitations of dynamical edge states: they do not survive in strongly curved environments; see Figure 6. This means that our results rely on κ being sufficiently regular. Other limitations include cross-type or knot-type interfaces, for which κ degenerates quadratically; see Figure 8. In both cases, the wavepackets seems to spread along Γ. This corresponds to a scattering process to other edge modes, that decay along Γ but have varying dispersion relations. Such scenarios form interesting open problems.

4.1. Proof of Theorem 4. The proof of Theorem 4 relies on the precise calculation of the corrector $a_1 = b_1 + \mathcal{K}_t f_1$ involved in sections 3.4–3.5.

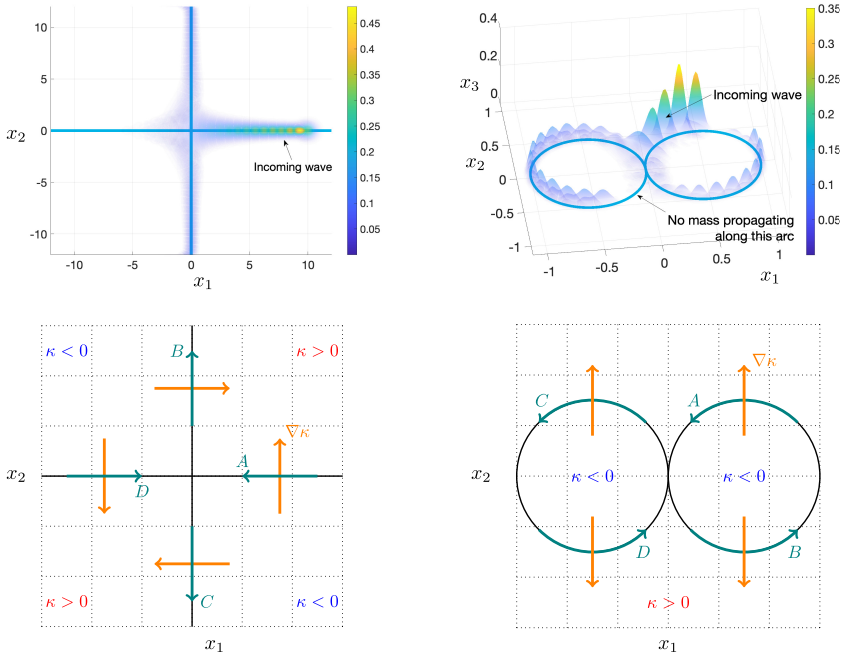

FIG. 8. *Top left: interface* $\kappa(x) = x_1 x_2$; *top right: an interface consisting of two rings;* $\kappa(x) = (|x + e_1| - 1)(|x - e_1| - 1)$, *both with* $\varepsilon = 2 \cdot 10^{-2}$. *In both cases, edge states propagate in the direction obtained by rotating* $\nabla\kappa$ *(orange arrow) by* $\pi/2$ *(teal arrow). Starting in direction A, the wavepacket reaches the crossroad. Directions B and C are then allowed, while direction D is forbidden. Theorem* 2 *does not address this scenario, because* $\nabla\kappa(0) = 0$.

LEMMA 4.1. *In the setup of Theorem* 4*, the subleading amplitude* $a_1 = b_1 + \mathcal{K}_t f_1$ *satisfies*

$$b_1(t,x) = \frac{1-x_1^2}{2} x_2 e^{-\frac{x^2}{2}} \begin{bmatrix} e^{-i\theta_t/2} \\ -e^{i\theta_t/2} \end{bmatrix} \dot\theta_t, \quad f_1(t,x_1) = \frac{2x_1 - x_1^3}{2} e^{-\frac{x_1^2}{2}} \Theta_t. \tag{4.4}$$

Proof of Lemma 4.1. The proof relies on the hierarchy of transport equations studied in section 3.4. We use the notations introduced there, keeping in mind that $r_t = 1$ here.

We first compute b_1. From the initial condition (1.3),

$$a_0(0,x) = e^{-\frac{x^2}{2}} \begin{bmatrix} e^{-i\theta_0/2} \\ -e^{i\theta_0/2} \end{bmatrix}.$$

Hence $f_0(x_1) = e^{-x_1^2/2}$. Moreover b_1 is the unique solution in $\ker(T_0)^\perp$ to $T_0 b_1 + T_1 a_0 = 0$. With $q_t(x) = \langle x, \nabla^2 \kappa(y_t) x \rangle$, this equation reads

$$T_0 b_1 = -e^{-\frac{x^2}{2}} \left(D_t + \frac{q_t(x)}{2} \sigma_3 \right) \begin{bmatrix} e^{-i\theta_t/2} \\ -e^{i\theta_t/2} \end{bmatrix} = \frac{1}{2} e^{-\frac{x^2}{2}} \left(\dot\theta_t - q_t(x) \right) \begin{bmatrix} e^{-i\theta_t/2} \\ e^{i\theta_t/2} \end{bmatrix}, \tag{4.5}$$

where we used the identities (3.27). To find b_1, we use the operators U_{θ_t} and $\mathcal{R}_{\theta_t}$ introduced in (2.2), and we look for b_1 of the form

$$b_1 = \mathcal{R}_{\theta_t} U_{\theta_t} \begin{bmatrix} c_1 \\ c_2 \end{bmatrix}.$$

We take advantage of the relation $T_0 = L_{\theta_t,1} = \mathcal{R}_{\theta_t} U_{\theta_t} L_{0,1} U_{\theta_t}^{-1} \mathcal{R}_{\theta_t}^{-1}$ (see (3.13) and the beginning of the proof of Lemma 3.2) and apply the operator $U_{\theta_t}^{-1} \mathcal{R}_{\theta_t}^{-1}$ to (4.5). We deduce that c_1 and c_2 must solve

$$L_{0,1} \begin{bmatrix} c_1 \\ c_2 \end{bmatrix} = \frac{1}{2} e^{-\frac{x^2}{2}} \left(\dot\theta_t - q_t\left(R_{\theta_t}^\top x\right) \right) U_{\theta_t}^{-1} \begin{bmatrix} e^{-i\theta_t/2} \\ e^{i\theta_t/2} \end{bmatrix} = \frac{1}{2} e^{-\frac{x^2}{2}} \left(\dot\theta_t - q_t\left(R_{\theta_t}^\top x\right) \right) \begin{bmatrix} 1 \\ 1 \end{bmatrix}.$$

We now use the operator $\tilde L_{0,1}$ of (3.18) and get

$$\begin{bmatrix} 0 & \mathfrak{a}^* & \mathfrak{a} & 2D_{x_1} \end{bmatrix} \begin{bmatrix} c_1 - c_2 \\ c_1 + c_2 \end{bmatrix} = e^{-\frac{x^2}{2}} \left(\dot\theta_t - q_t\left(R_{\theta_t}^\top x\right) \right) \begin{bmatrix} 0 \\ 1 \end{bmatrix}.$$

From $\mathfrak{a}^*(c_1 + c_2) = 0$, we obtain $c_1 = -c_2$ because $\mathfrak{a}^*$ has trivial kernel. Thus,

$$\begin{aligned} b_1(t,x) &= c_1(t, R_{\theta_t} x) U_{\theta_t} \begin{bmatrix} 1 \\ -1 \end{bmatrix} = c_1(t, R_{\theta_t} x) \begin{bmatrix} e^{-i\theta_t/2} \\ -e^{i\theta_t/2} \end{bmatrix}, \\ \mathfrak{a} c_1(t,x) &= \frac{1}{2} e^{-\frac{x^2}{2}} \left(\dot\theta_t - q_t\left(R_{\theta_t}^\top x\right) \right). \end{aligned}$$

We now use (4.2): $q_t(R_{\theta_t}^\top x) = \dot\theta_t x_1^2$. Hence c_1 satisfies the equation

$$\mathfrak{a} c_1(t,x) = \frac{1-x_1^2}{2} e^{-\frac{x^2}{2}} \dot\theta_t.$$

From the condition $b_1 \in \ker(T_0)^\perp$ we deduce that $c_1(t, x_1, \cdot) \perp e^{-x_2^2/2}$ for every (t, x_1). Therefore, c_1 is explicitly given by

$$c_1(t,x) = \frac{1-x_1^2}{2} \, x_2 \, e^{-\frac{x^2}{2}} \dot\theta_t. \tag{4.6}$$

This yields the identity (4.4) for b_1.

We now focus on f_1. It solves the transport equation (3.42)

$$D_t f_1(t,x_1) = \frac{1}{2\sqrt{\pi}} \int_{\mathbb{R}} e^{-\frac{x_2^2}{2}} \begin{bmatrix} e^{i\theta_t/2} \\ -e^{-i\theta_t/2} \end{bmatrix} \cdot \beta_1 \left(t, R_{\theta_t}^\top x\right) dx_2,$$

where by (3.41) $\beta_1 = -T_1 b_1 - T_2 a_0$. In view of (3.8), T_2 is carried by σ_3, and we deduce from (3.27) that

$$-\begin{bmatrix} e^{i\theta_t/2} \\ -e^{-i\theta_t/2} \end{bmatrix} \cdot \beta_1(t,x) = 2D_t\big(c_1(t,R_{\theta_t}x)\big) = 2\left(D_t + \dot{R}_{\theta_t} x \cdot D_x\right) c_1(t,R_{\theta_t}x).$$

Using (3.30), we obtain

$$\begin{aligned} -\begin{bmatrix} e^{i\theta_t/2} \\ -e^{-i\theta_t/2} \end{bmatrix} \cdot \beta_1(t,R_{\theta_t}^\top x) &= 2\left(D_t + \dot{R}_{\theta_t} R_{\theta_t}^\top x \cdot D_x\right) c_1(t,x) \\ &= 2\left(D_t + \dot{\theta}_t \begin{bmatrix} x_2 \\ -x_1 \end{bmatrix} \cdot D_x\right) c_1(t,x), \end{aligned}$$

hence the transport equation for f_1:

$$D_t f_1(t,x_1) = -\frac{1}{\sqrt{\pi}} \int_{\mathbb{R}} e^{-\frac{x_2^2}{2}} \left(D_t c_1(t,x) + \dot{\theta}_t (x_2 D_{x_1} - x_1 D_{x_2}) c_1(t,x)\right) dx_2. \tag{4.7}$$

Thanks to the explicit formula (4.6) for c_1, we have

$$\int_{\mathbb{R}} e^{-\frac{x_2^2}{2}} D_t c_1(t,x) dx_2 = \frac{1-x_1^2}{2} e^{-\frac{x_1^2}{2}} \int_{\mathbb{R}} x_2 e^{-\frac{x_2^2}{2}} dx_2 \cdot D_t \dot{\theta}_t = 0.$$

We deduce from integrating (4.7) and using the condition $f_1(0,x_1) = 0$ that

$$\begin{aligned} f_1(t,x_1) &= -\frac{1}{\sqrt{\pi}} \int_0^t \dot{\theta}_s \int_{\mathbb{R}} e^{-\frac{x_2^2}{2}} (x_2 \partial_{x_1} - x_1 \partial_{x_2}) c_1(s,x)\ dx_2\ ds \\ &= -\frac{1}{\sqrt{\pi}} \int_0^t \dot{\theta}_s \int_{\mathbb{R}} x_2 e^{-\frac{x_2^2}{2}} (\partial_{x_1} - x_1) c_1(s,x)\ dx_2\ ds, \end{aligned} \tag{4.8}$$

where we have performed an integration by parts in x_2. We now compute the integrals that appear in (4.8) using (4.6). The integral on the left-hand side corresponds to integrating an odd function and hence produces 0. Regarding the one on the RHS, we observe

$$(\partial_{x_1} - x_1) c_1(t,x) = x_2 (x_1^3 - 2x_1) e^{-\frac{x^2}{2}} \dot{\theta}_t.$$

Therefore, the RHS of (4.8) becomes

$$\begin{aligned} &\frac{1}{\sqrt{\pi}} \int_0^t \dot{\theta}_s \int_{\mathbb{R}} x_2 e^{-\frac{x_2^2}{2}} (\partial_{x_1} - x_1) c_1(s,x) dx_2 ds \\ &\quad = (x_1^3 - 2x_1) e^{-\frac{x_1^2}{2}} \int_0^t \dot{\theta}_s^2 ds \cdot \frac{1}{\sqrt{\pi}} \int_{\mathbb{R}} x_2^2 e^{-x_2^2} dx_2 \\ &\quad = \frac{2x_1 - x_1^3}{2} e^{-\frac{x_1^2}{2}} \int_0^t \dot{\theta}_s^2 ds. \end{aligned} \tag{4.9}$$

Plugging (4.9) in (4.8), we conclude that

$$f_1(t,x_1) = \frac{x_1^3 - 2x_1}{2} e^{-\frac{x_1^2}{2}} \Theta_t, \quad \text{where} \quad \Theta_t = \int_0^t \dot{\theta}_s^2 ds.$$

This completes the proof of Lemma 4.1. ∎

Proof of Theorem 4. We set $a^{(2)} = a_0 + \varepsilon^{1/2} a_1 + \varepsilon b_2$, with a_0, a_1, b_2 solutions of

$$T_0 a_0 = 0, \quad T_0 a_1 + T_1 a_0 = 0, \quad T_0 b_2 + T_1 a_1 + T_2 a_0 = 0;$$

see sections 3.4–3.7 for their construction. Thanks to Lemma 3.1, we have

$$\begin{aligned}&\left\|(\varepsilon D_t + H) W\left[a^{(2)}\right]_{y_t}\right\|_{L^2} \\ &\quad \le C\varepsilon^2 \left(\left\|D_t b_2\right\|_{L^2} + \left\|\langle x\rangle^4 a_0\right\|_{L^2} + \left\|\langle x\rangle^4 a_1\right\|_{L^2} + \left\|\langle x\rangle^4 b_2\right\|_{L^2}\right).\end{aligned}$$

From the explicit expression (3.33) for a_0, $\|\langle x\rangle^4 a_0\|_{L^2}$ is uniformly bounded. From the explicit expression (4.4) for a_1, $\|\langle x\rangle^4 a_1\|_{L^2}$ is bounded by $1 + \Theta_t$. It remains to bound $\|\langle x\rangle^4 b_2\|_{L^2}$ and $\|D_t b_2\|_{L^2}$. By construction, recalling that $r_t = 1$,

$$b_2(t,\cdot) = -L^{-1}_{\theta_t,1}\left(T_1 a_1 + T_2 a_0\right).$$

The explicit expressions for a_0 and a_1 allow us to bound Schwartz-class seminorms of $T_1 a_1 + T_2 a_0$ by $1 + \Theta_t$ (the term $\partial_t \Theta_t = (\partial_t \theta_t)^2$ is uniformly bounded). Arguing as in (3.38), we deduce that Schwartz-class seminorms of $b_2(t,\cdot)$ and $D_t b_2(t,\cdot)$ are bounded by $1 + \Theta_t$. In particular,

$$\left\|D_t b_2\right\|_{L^2} + \left\|\langle x\rangle^4 b_2\right\|_{L^2} \le C(1 + \Theta_t).$$

We deduce that

$$\left\|(\varepsilon D_t + H) W\left[a^{(2)}\right]_{y_t}\right\|_{L^2} \le C\varepsilon^2 \left(1 + \Theta_t\right).$$

We note that at $t = 0$, Ψ_t and $W[a^{(2)}]_{y_t}$ coincide up to $\mathcal{O}_{L^2}(\varepsilon^{1/2})$. Thus, applying Lemma 3.5, we conclude that

$$\left\|\Psi_t - W\left[a^{(2)}\right]_{y_t}\right\|_{L^2} \le C\varepsilon^{1/2} + C\varepsilon t \left(1 + \Theta_t\right).$$

This completes the proof of Theorem 4. ∎

4.2. Geometric setup. We prove here the geometric facts stated above. First, if Γ is a nodal set, then we can find a function κ satisfying (4.1) with $\kappa^{-1}(0) = \Gamma$.

LEMMA 4.2. *If $\Gamma = \tilde{\kappa}^{-1}(0)$ for a function $\tilde{\kappa} \in C^\infty(\mathbb{R}^2)$ satisfying $\nabla\tilde{\kappa} \in C^\infty_b(\mathbb{R}^2)$ and the transversality condition* (3.1)*, then we can find $\kappa \in C^\infty(\mathbb{R}^2)$ satisfying $\nabla\kappa \in C^\infty_b(\mathbb{R}^2)$ and* (4.1)*, such that moreover $\Gamma = \kappa^{-1}(0)$.*

Proof of Lemma 4.2. Without loss of generalities, we may replace $\tilde{\kappa}$ by

$$\frac{\tilde{\kappa}}{|\nabla\tilde{\kappa}|(1 + \tilde{\kappa}^2)}.$$

This means that we can assume that $\tilde{\kappa} \in C^\infty_b(\mathbb{R}^2)$ and $|\nabla\tilde{\kappa}(y)| = 1$ along Γ. We now aim to construct $\rho \in C^\infty_b(\mathbb{R}^2)$ with $|\tilde{\kappa}\rho|_\infty < 1$ such that if

$$\kappa = \tilde{\kappa} - \rho\frac{\tilde{\kappa}^2}{2} = \tilde{\kappa}\left(1 - \frac{\tilde{\kappa}\rho}{2}\right), \tag{4.10}$$

then κ satisfies (4.1). Under the condition $|\kappa\rho|_\infty < 1$, $\kappa^{-1}(0) = \tilde{\kappa}^{-1}(0) = \Gamma$. Moreover,

$$\nabla\kappa = \nabla\tilde{\kappa}\left(1 - \rho\tilde{\kappa}\right) - \frac{\tilde{\kappa}^2}{2}\nabla\rho;$$

hence if $y \in \Gamma$, then $\nabla\kappa(y) = \nabla\tilde{\kappa}(y)$. Also

$$\nabla^2\kappa = \nabla^2\tilde{\kappa}(1-\rho\tilde{\kappa}) - \rho\nabla\tilde{\kappa}\nabla\tilde{\kappa}^\top - \tilde{\kappa}\nabla\rho\nabla\kappa^\top - \tilde{\kappa}\nabla\tilde{\kappa}\nabla\rho^\top - \frac{\tilde{\kappa}^2}{2}\nabla^2\rho.$$

So, if $y \in \Gamma$, then $\nabla^2\kappa(y) = \nabla^2\tilde{\kappa}(y) - \rho(y)\nabla\tilde{\kappa}(y)\nabla\tilde{\kappa}(y)^\top$. We deduce that, for $y \in \Gamma$,

$$\begin{aligned}\left\langle \nabla\kappa(y), \nabla^2\kappa(y)\nabla\kappa(y)\right\rangle &= \left\langle \nabla\tilde{\kappa}(y), \nabla^2\tilde{\kappa}(y)\nabla\tilde{\kappa}(y)\right\rangle - \rho(y)\left\langle \nabla\tilde{\kappa}(y), \nabla\tilde{\kappa}(y)\nabla\tilde{\kappa}(y)^\top\nabla\tilde{\kappa}(y)\right\rangle \\ &= \left\langle \nabla\tilde{\kappa}(y), \nabla^2\tilde{\kappa}(y)\nabla\tilde{\kappa}(y)\right\rangle - \rho(y).\end{aligned}$$

We now pick $\tilde{\rho} \in C^\infty(\mathbb{R}^2)$ such that $\tilde{\rho}(y) = \langle \nabla\tilde{\kappa}(y), \nabla^2\tilde{\kappa}(y)\nabla\tilde{\kappa}(y)\rangle$ for $y \in \Gamma$. Then, with

$$\rho(y) = \frac{\tilde{\rho}(y)}{1+\tilde{\rho}(y)^2\tilde{\kappa}(y)^2},$$

we still have $\rho(y) = \langle \nabla\tilde{\kappa}(y), \nabla^2\tilde{\kappa}(y)\nabla\tilde{\kappa}(y)\rangle$ for $y \in \Gamma$; $\rho \in C_b^\infty(\mathbb{R}^2)$, and finally,

$$|\rho\tilde{\kappa}| = \frac{|\tilde{\rho}\tilde{\kappa}|}{1+\tilde{\rho}^2\tilde{\kappa}^2} \le \frac{1}{2}.$$

The function κ given by (4.10) now satisfies the requirements of the lemma. Indeed, by construction we have for $y \in \Gamma$

$$\left|\nabla\kappa(y)\right| = \left|\nabla\tilde{\kappa}(y)\right| = 1, \quad \left\langle \nabla\kappa(y), \nabla^2\kappa(y)\nabla\kappa(y)\right\rangle = 0. \tag{4.11}$$

We can then write $|\nabla\kappa|^2 = 1 + \alpha\kappa$ for some smooth function α. Taking the gradient on both sides produces the identity

$$2\nabla^2\kappa\cdot\nabla\kappa = \alpha\nabla\kappa + \kappa\nabla\alpha.$$

In particular, pairing with $\nabla\kappa^\perp$ gives

$$2\left\langle \nabla\kappa^\perp, \nabla^2\kappa\cdot\nabla\kappa\right\rangle = \kappa\left\langle \nabla\kappa^\perp, \nabla\alpha\right\rangle.$$

Specializing at $y \in \Gamma$ produces

$$\left\langle \nabla\kappa(y)^\perp, \nabla^2\kappa(y)\cdot\nabla\kappa(y)\right\rangle = 0,$$

which together with the second identity of (4.11) yields $\nabla^2\kappa(y)\nabla\kappa(y) = 0$ when $y \in \Gamma$. ∎

We now prove the useful relation (4.2).

Proof of (4.2). We recall that $R_{\theta_t}^\top e_1 = -\dot{y}_t = -\nabla\kappa(y_t)^\perp$ and $R_{\theta_t}^\top e_2 = -\dot{y}_t{}^\perp = \nabla\kappa(y_t)$. Therefore, proving (4.2) boils down to showing

$$\left\langle \dot{y}_t, \nabla^2\kappa(y_t)\dot{y}_t\right\rangle = \dot{\theta}_t, \quad \left\langle \dot{y}_t, \nabla^2\kappa(y_t)\dot{y}_t{}^\perp\right\rangle = 0, \quad \left\langle \dot{y}_t{}^\perp, \nabla^2\kappa(y_t)\dot{y}_t{}^\perp\right\rangle = 0. \tag{4.12}$$

The last two identities are direct consequences of $\nabla^2\kappa(y)\nabla\kappa(y) = 0$ for $y \in \kappa^{-1}(0)$. For the first identity in (4.12), we note that

$$\begin{cases} \cos(\theta_t) = -\left\langle \dot{y}_t, e_1\right\rangle = \left\langle \nabla\kappa(y_t), e_2\right\rangle, \\ \sin(\theta_t) = -\left\langle \dot{y}_t, e_2\right\rangle = -\left\langle \nabla\kappa(y_t), e_1\right\rangle. \end{cases}$$

Taking time derivatives, and the identity $\sin(\theta_t)e_2 + \cos(\theta_t)e_1 = -\dot{y}_t$, we deduce that

$$\begin{cases} \dot{\theta}_t \sin(\theta_t) = -\left\langle \nabla^2\kappa(y_t)\dot{y}_t, e_2 \right\rangle \\ \dot{\theta}_t \cos(\theta_t) = -\left\langle \nabla^2\kappa(y_t)\dot{y}_t, e_1 \right\rangle \end{cases} \quad \Rightarrow \quad \dot{\theta}_t = \left\langle \nabla^2\kappa(y_t)\dot{y}_t, \dot{y}_t \right\rangle .$$

This completes the proof of (4.2). ∎

Acknowledgments. This work started during the AIM workshop Mathematics of topological insulators. The authors gracefully thank the organizers: Daniel Freed, Gian Michele Graf, Rafe Mazzeo, and Michael Weinstein. They also thank Mitchell Luskin and Clément Tauber for interesting discussions.

REFERENCES

[1] J. E. Avron, R. Seiler, and B. Simon, *Quantum Hall effect and the relative index for projections*, Phys. Rev. Lett., 65 (1990), 2185.
[2] G. Bal, *Continuous bulk and interface description of topological insulators*, J. Math. Phys., 60 (2019), 081506.
[3] G. Bal, *Topological protection of perturbed edge states*, Commun. Math. Sci., 17 (2019), pp. 193–225.
[4] G. Bal, *Semiclassical Propagation Along Curved Domain Walls*, preprint, arXiv:2206.09439, 2022.
[5] G. Bal, *Topological invariants for interface modes*, Comm. Partial Differential Equations, 47 (2022), pp. 1636–1679.
[6] J. Bellissard, A. van Elst, and H. Schulz-Baldes, *The noncommutative geometry of the quantum Hall effect*, J. Math. Phys., 35 (1994), pp. 5373–5451.
[7] R. Bianco and R. Resta, *Mapping topological order in coordinate space*, Phys. Rev. B, 84 (2011), 241106, https://doi.org/10.1103/PhysRevB.84.241106.
[8] J. M. Bily and D. Robert, *The semi-classical Van Vleck formula. Application to the Aharonov-Bohm effect*, in Long Time Behaviour of Classical and Quantum Systems (Bologna, 1999), Ser. Concr. Appl. Math. 1, World Scientific Publishing, River Edge, NJ, 2001, pp. 89–106, https://doi.org/10.1142/9789812794598_0005.
[9] C.-Z. Chang, et al., *Experimental observation of the quantum anomalous Hall effect in a magnetic topological insulator*, Science, 340 (2013), pp. 167–170, https://doi.org/10.1126/science.1234414.
[10] Y. Colin de Verdière, *The level crossing problem in semi-classical analysis. II. The Hermitian case*, Ann. Inst. Fourier (Grenoble), 54 (2004), pp. 1423–1441.
[11] M. Combescure and D. Robert, *Coherent States and Applications in Mathematical Physics*, Springer, New York, 2012.
[12] A. Drouot, *The bulk-edge correspondence for continuous honeycomb lattices*, Comm. Partial Differential Equations, 44 (2019), pp. 1406–1430.
[13] A. Drouot, *Characterization of edge states in perturbed honeycomb structures*, Pure Appl. Anal., 1 (2019), pp. 385–445.
[14] A. Drouot, *Microlocal analysis of the bulk-edge correspondence*, Comm. Math. Phys., 383 (2021), pp. 2069–2112.
[15] A. Drouot, *Ubiquity of conical points in topological insulators*, J. Éc. Polytech. Math., 8 (2021), pp. 507–532.
[16] A. Drouot, *Topological Insulators in Semiclassical Regime*, preprint, arXiv:2206.08238, 2022.
[17] P. Elbau and G.-M. Graf, *Equality of bulk and edge Hall conductance revisited*, Comm. Math. Phys., 229 (2002), pp. 415–432.
[18] C. L. Fefferman, J. P. Lee-Thorp, and M. I. Weinstein, *Edge states in honeycomb structures*, Ann. PDE, 2 (2016), 12.
[19] C. Fermanian Kammerer, *A non-commutative Landau-Zener formula*, Math. Nachr., 271 (2004), pp. 22–50, https://doi.org/10.1002/mana.200310180.
[20] C. Fermanian Kammerer, *Semiclassical analysis of generic codimension 3 crossings*, Int. Math. Res. Not. IMRN, (2004), pp. 2391–2435, https://doi.org/10.1155/S1073792804133175.
[21] C. Fermanian Kammerer and P. Gérard, *A Landau-Zener formula for non-degenerated involutive codimension three crossings*, Ann. Henri Poincaré, 4 (2003), pp. 123–168.

[22] C. Fermanian-Kammerer, C. Lasser, and D. Robert, *Propagation of wave packets for systems presenting codimension one crossings*, Comm. Math. Phys., 385 (2021), pp. 1695–1739, https://doi.org/10.1007/s00220-021-04147-2.
[23] M. Fruchart and D. Carpentier, *An introduction to topological insulators*, C. R. Phys., 14 (2013), pp. 779–815.
[24] P. Gérard, P. A. Markowich, N. J. Mauser, and F. Poupaud, *Homogenization limits and Wigner transforms*, Comm. Pure Appl. Math., 50 (1997), pp. 323–379.
[25] P. Gérard, P. A. Markowich, N. J. Mauser, and F. Poupaud, *Erratum: "Homogenization limits and Wigner transforms" [Comm. Pure Appl. Math.* 50 *(*1997*), no.* 4, 323-379; *MR*1438151 (98d:35020)*]*, Comm. Pure Appl. Math., 53 (2000), pp. 280–281.
[26] G.-M. Graf, H. Jud, and C. Tauber, *Topology in shallow-water waves: A violation of bulk-edge correspondence*, Comm. Math. Phys., 383 (2021), pp. 731–761, https://doi.org/10.1007/s00220-021-03982-7.
[27] G.-M. Graf and M. Porta, *Bulk-edge correspondence for two-dimensional topological insulators*, Comm. Math. Phys., 324 (2013), pp. 851–895, https://doi.org/10.1007/s00220-013-1819-6.
[28] G. A. Hagedorn, *Molecular Propagation through Electron Energy Level Crossings*, Mem. Amer. Math. Soc. 111, Providence, RI, 1994.
[29] A. Haim, R. Ilan, and J. Alicea, *Quantum anomalous parity Hall effect in magnetically disordered topological insulator films*, Phys. Rev. Lett., 123 (2019), 046801, https://doi.org/10.1103/PhysRevLett.123.046801.
[30] F. D. M. Haldane, *Model for a quantum Hall effect without Landau levels: Condensed-matter realization of the parity anomaly*, Phys. Rev. Lett., 61 (1988), pp. 2015–2018, https://doi.org/10.1103/PhysRevLett.61.2015.
[31] Y. Hatsugai, *Chern number and edge states in the integer quantum Hall effect*, Phys. Rev. Lett., 71 (1993), pp. 3697–3700, https://doi.org/10.1103/PhysRevLett.71.3697.
[32] P. Z. Y. Hu and P. Xie, *Traveling edge states in massive dirac equations along slowly varying edges*, IMA J. Appl. Math., 2023, https://doi.org/10.1093/imamat/hxad015.
[33] P. Jurkowski and B. Szafran, *Persistent currents in topological and trivial confinement in silicene*, Phys. Rev. B, 101 (2020), 075408, https://doi.org/10.1103/PhysRevB.101.075408.
[34] J. Kellendonk, T. Richter, and H. Schulz-Baldes, *Edge current channels and chern numbers in the integer quantum Hall effect*, Rev. Math. Phys., 14 (2002), pp. 87–119, https://doi.org/10.1142/S0129055X02001107.
[35] A. Kitaev, *Anyons in an exactly solved model and beyond*, Ann. Phys., 321 (2006), pp. 2–111, https://doi.org/10.1016/j.aop.2005.10.005.
[36] J. P. Lee-Thorp, M. I. Weinstein, and Y. Zhu, *Elliptic operators with honeycomb symmetry: Dirac points, edge states and applications to photonic graphene*, Arch. Ration. Mech. Anal., 232 (2019), pp. 1–63.
[37] J. Liu and X. Dai, *Anomalous Hall effect, magneto-optical properties, and nonlinear optical properties of twisted graphene systems*, Comput. Math., 6 (2020), 57.
[38] T. A. Loring, *KK-theory and pseudospectra for topological insulators*, Ann. Phys., 356 (2015), pp. 383–416.
[39] T. A. Loring and H. Schulz-Baldes, *The spectral localizer for even index pairings*, J. Noncommut. Geom., 14 (2020), pp. 1–23.
[40] L. Lu, J. D. Joannopoulos, and M. Soljačić, *Topological photonics*, Nat. Photon., 8 (2014), pp. 821–829, https://doi.org/10.1038/nphoton.2014.248.
[41] A. Martinez and V. Sordoni, *Twisted Pseudodifferential Calculus and Application to the Quantum Evolution of Molecules*, Mem. Amer. Math. Soc. 936, American Mathematical Society, Providence, RI, 2009.
[42] V. Peano, C. Brendel, M. Schmidt, and F. Marquardt, *Topological phases of sound and light*, Phys. Rev. X, 5 (2015), 031011, https://doi.org/10.1103/PhysRevX.5.031011.
[43] E. Prodan and H. Schulz-Baldes, *Bulk and Boundary Invariants for Complex Topological Insulators: From K-Theory to Physics*, Springer, Berlin, 2016.
[44] S. Raghu and F. D. M. Haldane, *Analogs of quantum-Hall-effect edge states in photonic crystals*, Phys. Rev. A, 78 (2008), 033834, https://doi.org/10.1103/PhysRevA.78.033834.
[45] M. C.Rechtsman, et al., *Photonic Floquet topological insulators*, in Active Photonic Materials Vol. 880815, SPIE, Bellingham, WA, 2013, https://doi.org/10.1117/12.2023842.
[46] B. Simon, *Holonomy, the quantum adiabatic theorem, and Berry's phase*, Phys. Rev. Lett., 51 (1983), pp. 2167–2170, https://doi.org/10.1103/PhysRevLett.51.2167.
[47] E. M. Spanton, et al., *Observation of fractional Chern insulators in a van der Waals heterostructure*, Science, 360 (2018), pp. 62–66, https://doi.org/10.1126/science.aan8458.
[48] S. Teufel, *Adiabatic Perturbation Theory in Quantum Dynamics*, Lecture Notes in Mathematics 1821, Springer, Berlin, 2003, https://books.google.ch/books?id=zAzoqX3wFSIC.

[49] G. E. Volovik, *Nonlinear phenomena in condensed matter: Universe in a helium droplet*, in Nonlinear Waves 2, A. V. Gaponov-Grekhov, M. I. Rabinovich, J. Engelbrecht, eds., Springer-Verlag, Berlin, 1989, pp. 118–127.
[50] E. Witten, *Three lectures on topological phases of matter*, Nuovo Cimento Rivista Serie, 39 (2016), pp. 313–370, https://doi.org/10.1393/ncr/i2016-10125-3.
[51] M. Zworski, *Semiclassical Analysis*, Grad. Stud. Math., American Mathematical Society, Providence, RI, 2012.